[18] K.J. Mather, S. Verma, T.J. Anderson, Improved endothelial function with metformin in type 2 diabetes mellitus, J. Am. Coll. Cardiol. 37 (2001) 1344–1350.

[19] E. Karatzis, J. Lekakis, C. Papamichael, I. Andreadou, A. Cimponeriu, K. Aznaouridis, et al., Rapid effect of pravastatin on endothelial function and lipid peroxidation in unstable angina, Int. J. Cardiol. 101 (2005) 65–70.

[20] P. van der Harst, L.J. Wagenaar, H. Buikema, A.A. Voors, H.W. Plokker, W.J. Morshuis, et al., Effect of intensive versus moderate lipid lowering on endothelial function and vascular responsiveness to angiotensin II in stable coronary artery disease, Am. J. Cardiol. 96 (2005) 1361–1364.

[21] L.O. Jensen, P. Thayssen, K.E. Pedersen, T. Haghfelt, Short- and long-term influence of diet and sinvastatin on brachial artery endothelial function, Int. J. Cardiol. 107 (2006) 101–106.

[22] E. Corrado, I. Muratori, R. Tantillo, F. Contrno, G. Coppola, A. Strano, et al., Relationship between endothelial dysfunction, intima media thickness and cardiovascular risk factors in asymptomatic subjects, Int. Angiol. 24 (2005) 52–58.

[23] K. Noma, C. Goto, K. Nishioka, K. Hara, M. Kimura, T. Umemura, et al., Endothelial function, and Rho-kinase in humans, Arterioscler. Thromb. Vasc. Biol. 25 (2005) 2630–2635.

[24] X.L. Du, D. Edelstein, S. Dimmeler, Q. Ju, C. Sui, M. Brownlee, Hyperglycemia inhibits endothelial nitric oxide synthase activity by posttranslational modification at the Akt site, J. Clin. Invest. 108 (2001) 1341–1348.

[25] H. Kawano, T. Motoyama, O. Hirashima, N. Hirai, Y. Miyao, T. Sakamoto, et al., Hyperglycemia rapidly suppresses flow-mediated endothelium-dependent vasodilation of brachial artery, J. Am. Coll. Cardiol. 31 (1999) 146–154.

[26] F. Pistrosch, K. Fuecker, J. Passauer, M. Hanefeld, S. Fischer, P. Gross, In type 2 diabetes, rosiglitazone therapy for insulin resistance ameliorates endothelial dysfunction independent of glucose control, Diabetes Care 27 (2004) 484–490.

# Undernutrition *in Utero* Augments Systolic Blood Pressure and Cardiac Remodeling in Adult Mouse Offspring: Possible Involvement of Local Cardiac Angiotensin System in Developmental Origins of Cardiovascular Disease

Makoto Kawamura, Hiroaki Itoh, Shigeo Yura, Haruta Mogami, Shin-Ichi Suga, Hisashi Makino, Yoshihiro Miyamoto, Yasunao Yoshimasa, Norimasa Sagawa, and Shingo Fujii

*Department of Gynecology and Obstetrics (M.K., H.I., S.Y., H.Mo., S.F.), Kyoto University Graduate School of Medicine, Kyoto 606-8507, Japan; Departments of Etiology and Pathology (S.-I.S.) and Atherosclerosis and Diabetes (H.Ma., Y.M., Y.Y.), National Cardiovascular Center, Suita, Osaka 565-8565, Japan; Department of Obstetrics and Gynecology (N.S.), Mie University Graduate School of Medicine, Tsu, Mie 514-8507, Japan; and Precursory Research for Embryonic Science and Technology (PRESTO) (S.Y.), Japan Science and Technology Agency (JST), Kawaguchi City, Saitama 332-0012, Japan*

Evidence has emerged that undernutrition *in utero* is a risk factor for cardiovascular disorders in adulthood, along with genetic and environmental factors. Recently, the local expression of angiotensinogen and related bioactive substances has been demonstrated to play a pivotal role in cardiac remodeling, *i.e.* fibrosis and hypertrophy. The aim of the present study was to clarify the possible involvement of the local cardiac angiotensin system in fetal undernutrition-induced cardiovascular disorders. We developed a mouse model of undernutrition *in utero* by maternal food restriction, in which offspring (UN offspring) showed an increase in systolic blood pressure (8 wk of age, $P < 0.05$; and 16 wk, $P < 0.01$), perivascular fibrosis of the coronary artery (16 wk, $P < 0.05$) and cardiac cardiomegaly (16 wk, $P < 0.01$), and cardiomyocyte enlargement, concomitant with a significant augmentation of angiotensinogen ($P < 0.05$) and endothelin-1 ($P < 0.01$) mRNA expression and a tendency to increase in immunostaining for both angiotensin II and endothelin-1 in the left ventricles (16 wk). These findings suggest that fetal undernutrition activated the local cardiac angiotensin system-associated bioactive substances, which contributed, at least partly, to the development of cardiac remodeling in later life, in concert with the effects of increase in blood pressure. (*Endocrinology* 148: 1218–1225, 2007)

---

IN THE EARLY 1990s, a novel hypothesis was advanced by Barker *et al.* (1) to link nutritional insults during embryonic and fetal periods not only to impaired maturation of physiological functions, but also to cardiovascular diseases in adulthood. Alterations in nutrition and endocrine status during the embryonic, fetal, and neonatal periods can trigger developmental predictive adaptive responses (2), causing permanent structural, physiological, and metabolic changes, thereby predisposing an individual to cardiovascular, metabolic, and endocrine diseases in adult life.

The renin-angiotensin system (RAS) plays an important role in primary as well as secondary forms of hypertension in both animals and humans (3). More recently, components

of the RAS, such as angiotensin-converting enzyme (ACE) and angiotensin II, were revealed to be produced locally in the cardiac tissues, and termed the local cardiac RAS (4), being primary candidates for the factors promoting cardiac remodeling, mainly cardiac myocyte hypertrophy and increased extracellular matrix fibrosis, thereby deteriorating cardiac function (5). Various experimental animal models have been developed to investigate the associations between fetal undernutrition and cardiovascular disease later in life (6, 7), and a possible commitment of a systemic RAS in the developmental origins of hypertension was reported (8). Therefore, the aim of the present study was to investigate whether the local cardiac RAS is associated with the developmental origins of cardiac remodeling in offspring exposed to undernutrition *in utero*.

Recently, we developed a mouse model of undernutrition *in utero* using maternal food restriction, in which the offspring (UN offspring) developed pronounced obesity when fed a high-fat diet, accompanied by impaired hypothalamic leptin sensitivity, as compared with normally nourished offspring (NN offspring) (9). Using this model, we investigated whether fetal undernutrition affects systolic blood pressure (SBP), cardiac remodeling, and expression of local cardiac RAS-associated bioactive substances. We found that undernutrition *in utero* caused a significant increase in SBP as well

1218

as cardiac remodeling, concomitant with a significant elevation in mRNA expression in angiotensinogen (Ang) and endothelin-1 (ET-1) in the left ventricle.

## Materials and Methods

### Development of a mouse model of undernutrition in utero

Undernutrition *in utero* by maternal food restriction was carried out as described previously (9). In brief, pregnant C57Bl/6 mice were purchased at 8.5 d postcoitum (dpc) from Japan Central Laboratories for Experimental Animals (Tokyo, Japan) and were divided into two groups at 10.5 dpc. Dams were housed individually with free access to water during 14-h light, 10-h dark cycles. The daily food supply of one group was restricted to 70% of the food consumed by the other group, fed *ad libitum*, based on the data of the previous day, from 10.5 dpc to the day of delivery of the pups. Dams of the food restriction group were supplied 2.5 g of extra food in the evening of 18.5 dpc, just before the night of parturition, to prevent mothers from eating their own pups. Pups were nursed by mothers fed *ad libitum* (eight pups per mother) and were weaned on to regular chow diet (RCD; Oriental Yeast Co., Tokyo, Japan) at 21.5 d of age. RCD includes 20.8% protein and 4.8% fat, with contents of sodium (0.19 g/100 g) and potassium (0.75 g/100 g). Only male pups were used for the following experiments, except for the study of fetal heart tissues. Each group in all experiments consists of offspring from at least four litters. All experimental procedures were approved by the Animal Research Committee, Kyoto University Graduate School of Medicine (Med Kyo 64116).

### Measurement of SBP

At 4, 8, and 16 wk of age, SBP was measured at least five times in conscious mice (n = 8–10 for each group) using an indirect tail-cuff method (MK-2000; Muromachi Kikai Co. Ltd., Tokyo, Japan).

### Neonatal leptin or monosodium glutamate treatment

Leptin (2.5 µg/g body weight·d) (PeproTech Inc., Rocky Hill, NJ) or vehicle saline was sc administered to NN offspring daily from 5.5 to 10.5 d of age, as a model of premature leptin surge (9), then SBP was measured at 8 wk. Monosodium glutamate (2 mg/g body weight·d) was sc administered to NN and UN offspring from 1.5 to 5.5 d of age, as previously described (9), for the purpose of permanent chemical injury of the arcuate nucleus of the hypothalamus (ARC) (10), then SBP was measured at 16 wk.

### Morphological analysis of the kidney

For morphological analysis, whole kidneys were sampled at 8 and 16 wk, weighed and fixed in 10% formalin, and embedded in paraffin. The kidneys were cut into sections 2-µm thick and stained with hematoxylin and eosin, periodic-acid Schiff (PAS), or Masson trichrome. The stained sections were analyzed light microscopically.

### Serum nitrite/nitrate (NOx) and plasma angiotensin II concentration

NOx concentration was determined by the Griess reaction using a commercial colorimetric assay kit (Cayman Chemical, Ann Arbor, MI). The angiotensin II concentration was determined with an ELISA kit (Peninsula Laboratories, Belmont, CA), after extraction through $C_{18}$ Sep-Pak columns (Waters Co., Milford, MA).

### Urine microalbumin concentration

Urine was collected for 24 h using metabolic cages, and microalbuminuria was determined by the competitive ELISA method (Albuwell M assay kit; Exocell, Philadelphia, PA) at 16 wk of age. Urine creatinine values were assessed simultaneously by enzyme assay (MIZUHO MEDY Co., Ltd., Saga, Japan) and were used to calculate the albumin to creatinine ratio.

### Morphometric analysis of the heart

The whole hearts were sampled, fixed in 10% formalin, and embedded in paraffin at 8 and 16 wk. The heart was cut into two subserial cross-sections 6-µm thick at intervals of 1 mm and stained with Sirius Red to evaluate the perivascular fibrosis of coronary arteries 100–200 µm in diameter. The perivascular fibrosis was assessed by analyses of digital images, calculating the ratio of the area of Sirius Red-stained fibrosis to the total vessel area using a KS400 image system (Zeiss, Oberkochen, Germany). To evaluate perivascular fibrosis in renal small arteries 100–200 µm in diameter, the kidneys were also sampled in the offspring at 16 wk and evaluated in the same manner as the coronary arteries.

To determine the interstitial fibrosis of the heart at 16 wk of age, we randomly selected 20 fields in two different sections and calculated the ratio of the areas of Sirius Red-stained interstitial fibrosis to the total cross-sectional areas.

Cardiomegaly was assessed by whole-heart weight to body weight ratio at 8 and 16 wk. Cardiomyocyte enlargement was estimated by measuring shortest transverse diameter in nucleated transverse sections of the myocytes. In each sample at 16 wk, 8 fields were randomly selected, and 80 cells were measured.

### Quantitative RT-PCR analysis

Total RNA was extracted from whole hearts of fetal mice at 18.5 dpc and from left ventricles of the mice at 3, 8, and 16 wk, as well as from kidneys at 16 wk. The mRNA expression was measured by real-time quantitative RT-PCR using Taqman technology (Model 7000 sequence detector; Applied Biosystems, Foster City, CA). The forward and reverse primers and Fam/Tamra or Fam/MGB probes used for the targeted amplification of part of the cDNAs of murine Ang, angiotensin II type 1 receptor (AT1R), angiotensin II type 2 receptor (AT2R), ACE, renin, ET-1, atrial natriuretic peptide (ANP), and brain natriuretic peptide (BNP) are summarized in Table 1. The forward and reverse primers and Joe/Tamra probes for the murine glyceraldehyde-3-phosphate dehydrogenase (GAPDH) and ribosomal RNA coding region were purchased from Applied Biosystems. Serial dilutions of total RNA sample, isolated from mouse left ventricles or kidneys, were used to construct the standard curve for each substance. The standard curves were calculated by linear regression analysis, and threshold cycle values were used to read off relative RNA amounts. An mRNA expression value was then obtained by dividing the value for the gene of interest by the value for the ribosomal RNA or GAPDH.

At first, we assessed expression of ribosomal RNA and GAPDH mRNA based on total RNA concentration assessed by optic densitometry. The fetal undernutrition significantly decreased ribosomal RNA expression, but not GAPDH mRNA expression, in the fetal heart (data not shown). By contrast, fetal undernutrition significantly decreased GAPDH mRNA expression, but not ribosomal RNA expression, in the left ventricle after birth (data not shown). Therefore, we used GAPDH and ribosomal RNA data for analyses in the fetal heart (18.5 dpc) and in the left ventricle after birth (3, 8, and 16 wk), respectively, to compensate the variation. Because fetal undernutrition did not change GAPDH mRNA expression in the adult kidney (data not shown), GAPDH data were used for analyses in the adult kidney.

### Immunohistochemistry of angiotensin II, ET-1, and renin

Six-micrometer-thick sections of the paraffin-embedded whole heart were incubated for overnight at 4 C with rabbit antiserum against angiotensin-II (1:500) (T-4007; Peninsula Laboratories), ET-1 (1:500) (T-4050; Peninsula Laboratories), or goat antiserum against renin (1:1600) (kindly donated by Professor Tadashi Inagami, Vanderbilt University School of Medicine, Nashville, TN) (11). Normal goat or rabbit serum (Dako Co., Carpinteria, CA) was used as negative controls. Staining was detected using an avidin-biotin-peroxidase method kit (ELITE ABC; Vector Laboratories, Burlingame, CA) with 3,3'-diaminobenzidine as previously described (12).

### Statistical analysis

Values were expressed as means ± SEM. The significance of differences was assessed with Student's *t* test. *P* values < 0.05 were regarded as significant.

**TABLE 1.** Forward/reverse primers and FAM/Tamra or FAM/MGB probes used in the quantitive PCR analysis

| | Primers (5'–3') |
|---|---|
| Ang | |
| Forward | CAGCACCCTACTTTTCAACACCTA |
| Reverse | TGTTGTCCACCCAGAATTCATG |
| FAM/MGB probe | TCCAAGGAACGATGAGAG |
| ACE | |
| Forward | AATCGGCCTACTGGACCATGT |
| Reverse | GGCCATCTTTAGCAGGTAATTGAT |
| FAM/MGB probe | ACCAATGACATAGAGAGTG |
| AT1R | |
| Forward | GATCGCTACCTGGCCATTGT |
| Reverse | GTGACTTTGGCCACCAGCAT |
| FAM/MGB probe | CCGATGAAGTCTCGC |
| AT2R | |
| Forward | TGCTGGGATTGCCTTAATGAA |
| Reverse | TCAGGACTTGGTCACGGGTAAT |
| FAM/MGB probe | AGCAACGTGTTACTTTG |
| Renin | |
| Forward | CACTACGGATCAGGGAGAGTCAA |
| Reverse | CAGCTCGGTGACCTCTCCAA |
| FAM/MGB probe | CAGGACTCGGTGACTGT |
| ET-1 | |
| Forward | CTTCTGCCACCTGGACATCAT |
| Reverse | TGGTGAGCGCACTGACATCTA |
| FAM/MGB probe | AGCGCGTCGTACCGTA |
| ANP | |
| Forward | GCCATATTGGAGCAAATCCT |
| Reverse | GCAGGTTCTTGAAATCCATCA |
| FAM/Tamra probe | TGTACAGTGCGGTGTCCAACACAGAT |
| BNP | |
| Forward | CCAGTCTCCAGAGCAATTCAA |
| Reverse | GCCATTTCCTCCGACTTTT |
| FAM/Tamra probe | TGCAGAAGCTGCTGGAGCTGATAAGA |

Ang, GenBank accession no. BC019496; Strausberg *et al.*, 2002. ACE, BC083109; Strausberg *et al.*, 2002. AT1R, BC036175; Strausberg *et al.*, 2002. AT2R, AK086334; Carninci *et al.*, 1999. Renin, NM_031192; Wilson *et al.*, 1977. ET-1, BC029547; Strausberg *et al.*, 2002. ANP, D70837; Tamura *et al.*, 1996. BNP, D82049; Ogawa *et al.*, 1994.

## Results

### SBP at 4, 8, and 16 wk

There was no significant difference in SBP between UN and NN offspring at 4 wk. However, the SBP of UN offspring was significantly higher than that of NN offspring at 8 wk ($P < 0.05$), and the elevation of SBP in UN offspring continued at least until 16 wk ($P < 0.01$) (Fig. 1A).

### SBP after neonatal leptin or monosodium glutamate treatment

There was no significant difference in SBP between NN offspring with neonatal leptin treatment (90.5 ± 1.4 mm Hg, n = 10) and those with neonatal vehicle treatment (86.3 ± 1.6 mm Hg, n = 10) at 8 wk. The significant elevation of SBP in UN offspring, as compared with NN offspring, at 16 wk was not blocked by chemical injury of the ARC by neonatal monosodium glutamate treatment (108.1 ± 5.2 mm Hg, n = 9 *vs.* 88.8 ± 5.0 mm Hg, n = 8; $P < 0.05$).

### Serum NOx concentration and plasma angiotensin II concentration

The serum NOx concentration of UN offspring was significantly lower than that of NN offspring at 8 wk ($P < 0.05$)
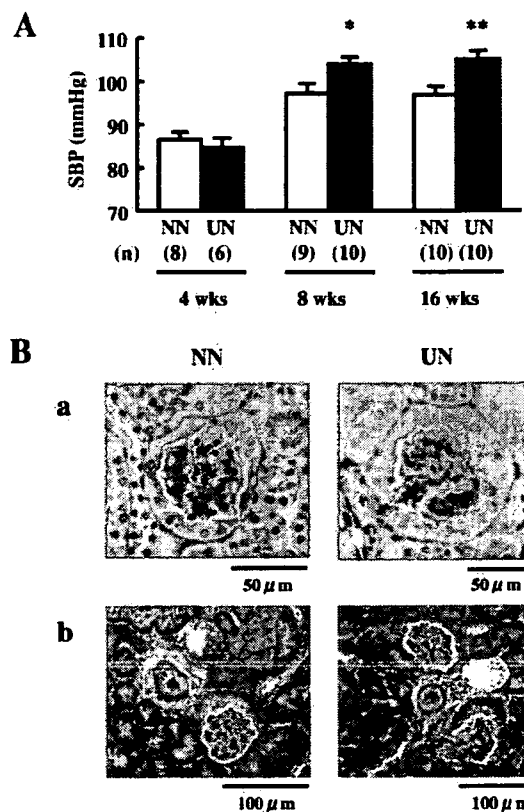


FIG. 1. SBP (A), PAS (Ba), and Masson trichrome (Bb) staining of kidney in NN offspring and UN offspring. *Columns* and *error bars* represent the mean and SEM of SBP. *, $P < 0.05$; **, $P < 0.01$ *vs.* NN offspring. Original magnification was ×400 (Ba) or ×200 (Bb). wks, Weeks of age.

(Table 2). Such a tendency was also observed at 16 wk, but the difference was not statistically significant (Table 2).

The plasma angiotensin II concentration of UN offspring was similar to that of NN offspring at 8 wk (Table 2). At 16 wk, the plasma angiotensin II concentration of UN offspring was higher than that of NN offspring, but the difference was not significant (Table 2).

### Urine microalbuminuria

There was no significant difference in urine microalbumin concentration between UN and NN offspring at 16 wk (25.03 ± 2.06 μg/mg creatinine, n = 7 *vs.* 22.52 ± 1.65 μg/mg creatinine, n = 8).

### Morphological analysis of the kidney

At 16 wk of age, the ratio of renal weight to body weight (mg/g) in UN offspring (5.58 ± 0.32, n = 20) was similar to that of in NN offspring (5.69 ± 0.27, n = 20).

Microscopic observation of hematoxylin and eosin (data not shown), PAS (Fig. 1Ba), and Masson trichrome (Fig. 1Bb) staining of kidneys from UN offspring at 8 and 16 wk showed no histological abnormalities as compared with NN offspring including nephron numbers.

**TABLE 2.** Serum NOx concentrations and plasma angiotensin II concentrations

| | 8 wk | | 16 wk | |
| --- | --- | --- | --- | --- |
| | NN | UN | NN | UN |
| NOx (μM) | 29.1 ± 3.1 (n = 9) | 19.0 ± 2.5$^a$ (n = 10) | 19.0 ± 2.8 (n = 10) | 14.2 ± 2.2 (n = 10) |
| Angiotensin II (pg/ml) | 43.3 ± 3.5 (n = 14) | 43.4 ± 4.9 (n = 11) | 118.9 ± 14.0 (n = 8) | 179.1 ± 38.7 (n = 8) |

Values are the mean ± SEM.
$^a$ $P < 0.05$ *vs.* NN.

### Perivascular fibrosis of the coronary artery and renal small artery

At 8 wk of age, the ratio of coronary perivascular fibrosis to total vessel area in UN offspring had tended to increase as compared with that in NN offspring; however, the difference was not significant (Fig. 2B). At 16 wk of age, the ratio of coronary perivascular fibrosis to total vessel area was significantly higher in the UN offspring than NN offspring ($P <$ 0.05) (Fig. 2, A and B). By contrast, the ratio of perivascular fibrosis to total vessel area in renal small arteries of UN offspring was similar to that in NN offspring at 16 wk of age (Fig. 2C).

### Interstitial fibrosis of the heart

Interstitial fibrosis of the heart in UN offspring at 16 wk was similar to that in NN offspring (Table 3A).
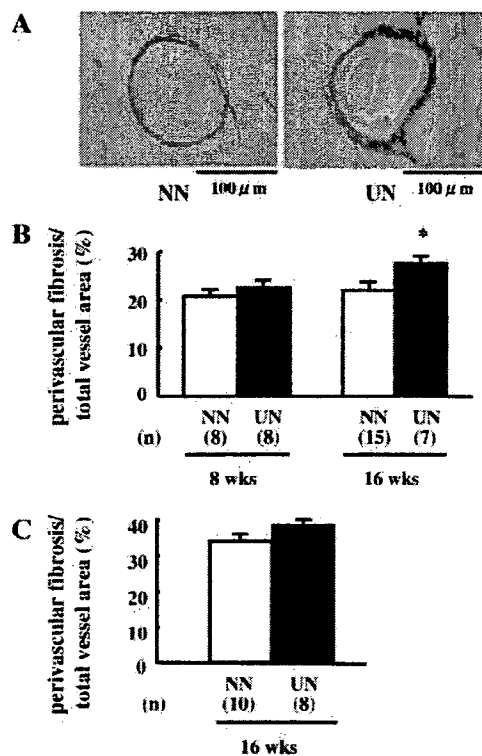


FIG. 2. Perivascular fibrosis in coronary and renal small arteries of NN and UN offspring. Representative cross-sections of coronary perivascular fibrosis at 16 wk of age (A). Collagen fibril was stained red with Sirius Red stain. Original magnification was ×400. Digital image analysis of perivascular fibrosis of coronary (B) and renal small arteries (C) as described in *Materials and Methods. Columns* and *error bars* represent the mean and SEM of the ratio of the area of Sirius Red-stained fibrosis to total vessel area (%). *, $P < 0.05$ *vs.* NN offspring. wks, Weeks of age.

### Cardiomegaly and cardiomyocyte enlargement

The ratio of heart weight to body weight and transverse diameter of the cardiomyocytes were significantly higher in the UN offspring than NN offspring at 16 wk ($P <$ 0.01) (Table 3B), in parallel with the increased perivascular fibrosis of coronary artery (Fig. 2B). However, cardiomegaly was not detected in UN offspring at 8 wk (Table 3B).

### The mRNA expression of local cardiac RAS-associated bioactive substances in the left ventricles at 3, 8, and 16 wk

There were no significant changes in Ang, ACE, AT1R, AT2R, ET-1, ANP, or BNP mRNA expression between NN and UN offspring at 3 wk (Figs. 3 and 4).

At 8 wk, a significant decrease was observed in Ang mRNA expression in UN offspring ($P <$ 0.01) (Fig. 3). By contrast, a significant increase was detected in AT2R ($P <$ 0.01), ET-1 ($P <$ 0.01), and BNP ($P <$ 0.01) (Figs. 3 and 4) at 8 wk; whereas ANP mRNA expression had a tendency to increase, but not significantly (Fig. 4).

At 16 wk, a significant increase was observed in the mRNA expression of Ang ($P <$ 0.05), AT2R ($P <$ 0.05), and ET-1 ($P <$ 0.01), but not in that of other substances (Figs. 3 and 4).

The renin mRNA expression in the left ventricles at 3, 8, and 16 wk was less than detection sensitivity of quantitative RT-PCR analysis (<0.00024-fold, compared with the whole kidney as a positive control).

### Immunohistochemistry of angiotensin II, ET-1, and renin in the left ventricle

Immunostaining of both angiotensin II and ET-1 were mainly observed in cardiomyocytes of the left ventricle at 16 wk (Fig. 5, A and B). There occurred a tendency to increase in immunostaining for angiotensin II as well as ET-1 in UN offspring, as compared with NN offspring (Fig. 5, A and B).

Immunohistochemistry detected a few renin positive cells (one to two cells per slide) in the perivascular interstitial area (Fig. 5C). There was no apparent difference in the renin staining between NN and UN offspring at 16 wk (Fig. 5C).

### The mRNA expression of local cardiac RAS-associated bioactive substances in the whole fetal heart at 18.5 dpc

A significant increase was observed in the mRNA expression of Ang ($P <$ 0.05), ACE ($P <$ 0.01), and ET-1 ($P <$ 0.05) in the whole fetal heart at 18.5 dpc, but not in that of other substances (Table 4).

### Discussion

In the present study, maternal food restriction caused a significant increase in SBP. However, neither the plasma

**TABLE 3.** Interstitial fibrosis of the heart (A) and cardiomegaly and cardiomyocyte enlargement (B)

| | 8 wk | | 16 wk | |
|---|---|---|---|---|
| | NN | UN | NN | UN |
| A. Interstitial fibrosis of the heart (%)[a] | | | 0.782 ± 0.041 (n = 15) | 0.751 ± 0.065 (n = 7) |
| B. Cardiomegaly and cardiomyocyte enlargement | | | | |
| HW (mg) | 127.1 ± 3.8 | 120.0 ± 3.0 | 158.9 ± 5.6 | 177.3 ± 6.2[b] |
| BW (g) | 23.9 ± 0.2 | 23.2 ± 0.3 | 31.4 ± 0.5 | 30.6 ± 0.5 |
| HW/BW (mg/g) | 5.31 ± 0.13 (n = 24) | 5.20 ± 0.14 (n = 19) | 5.05 ± 0.12 (n = 14) | 5.79 ± 0.18[c] (n = 16) |
| Cardiomyocyte diameter (μm) | | | 14.3 ± 0.3 (n = 10) | 16.6 ± 0.3[c] (n = 10) |

Values are the mean ± SEM. HW, Heart weight; BW, body weight.
[a] No significant difference.
[b] $P < 0.05$ vs. NN.
[c] $P < 0.01$ vs. NN.

angiotensin II concentration (Table 2) nor the microalbumin concentration in UN offspring produced significant changes, although basal plasma angiotensin II concentration at 16 wk was higher than other reports (13). A significant decrease in the plasma NOx concentration of UN offspring was observed

at 8 wk, as compared with that of NN offspring (Table 2). The decrease in the plasma NOx concentration of UN offspring was also observed at 16 wk, although it was not significant (Table 2). These observations suggested a possible involvement of endothelial dysfunction in the elevation of blood pressure in UN offspring, which is relevant to previous reports (14, 15). Histological examinations detected no abnormal findings in the renal tissues of UN offspring at 8 and 16 wk, although some investigators have demonstrated a possible involvement of small nephron numbers and/or a small number and size of glomeruli in increases in blood pressure during adulthood (16, 17).
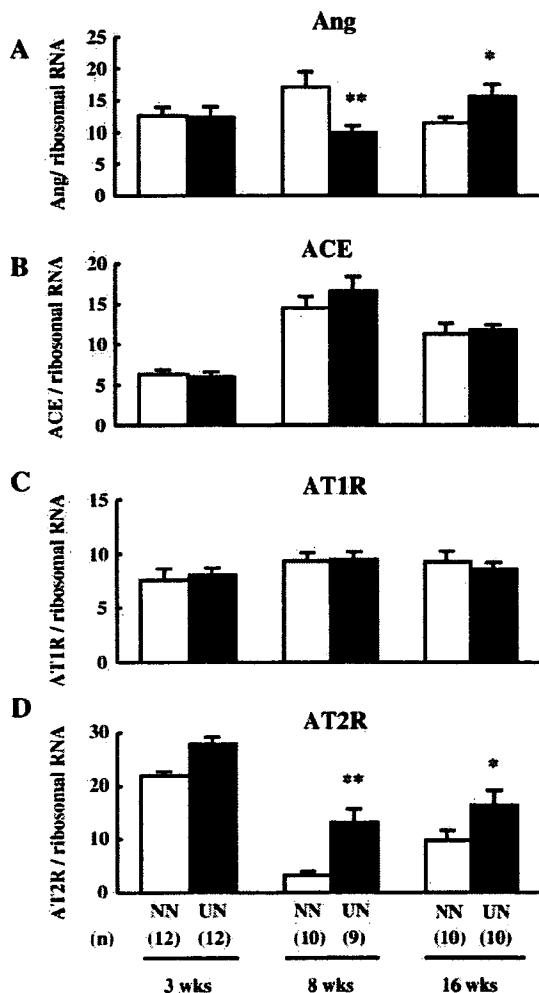


FIG. 3. The mRNA expression of Ang (A), ACE (B), AT1R (C), and AT2R (D) in the murine left ventricle at 3, 8, and 16 wk. *Columns* and *error bars* represent the mean and SEM of the mRNA expression in NN and UN offspring, measured by quantitative RT-PCR with real time TaqMan technology as described in *Materials and Methods.* *, $P < 0.01$; **, $P < 0.05$ vs. NN offspring. wks, Weeks of age.
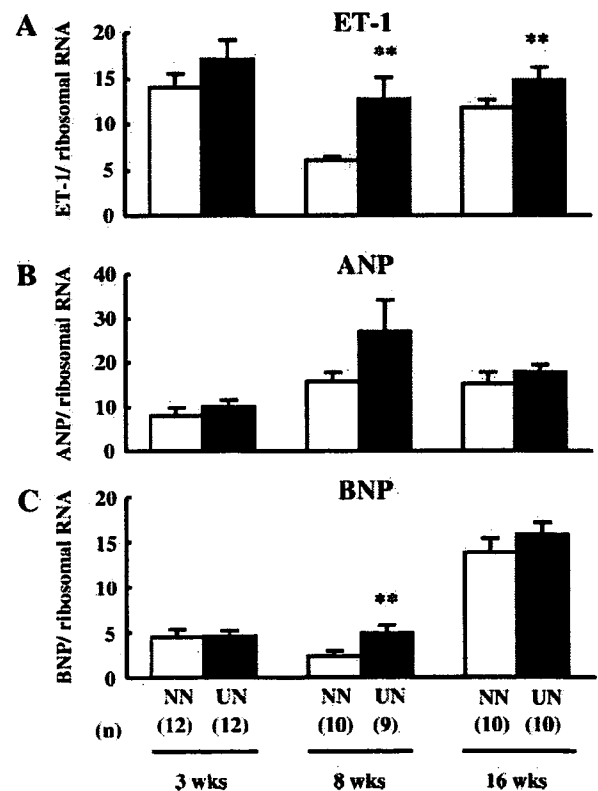


FIG. 4. The mRNA expression of ET-1 (A), ANP (B), and BNP (C) in the murine left ventricle at 3, 8, and 16 wk. *Columns* and *error bars* represent the mean and SEM of the mRNA expression in NN and UN offspring measured by quantitative RT-PCR with real time TaqMan technology as described in *Materials and Methods.* **, $P < 0.01$ vs. NN offspring. wks, Weeks of age.
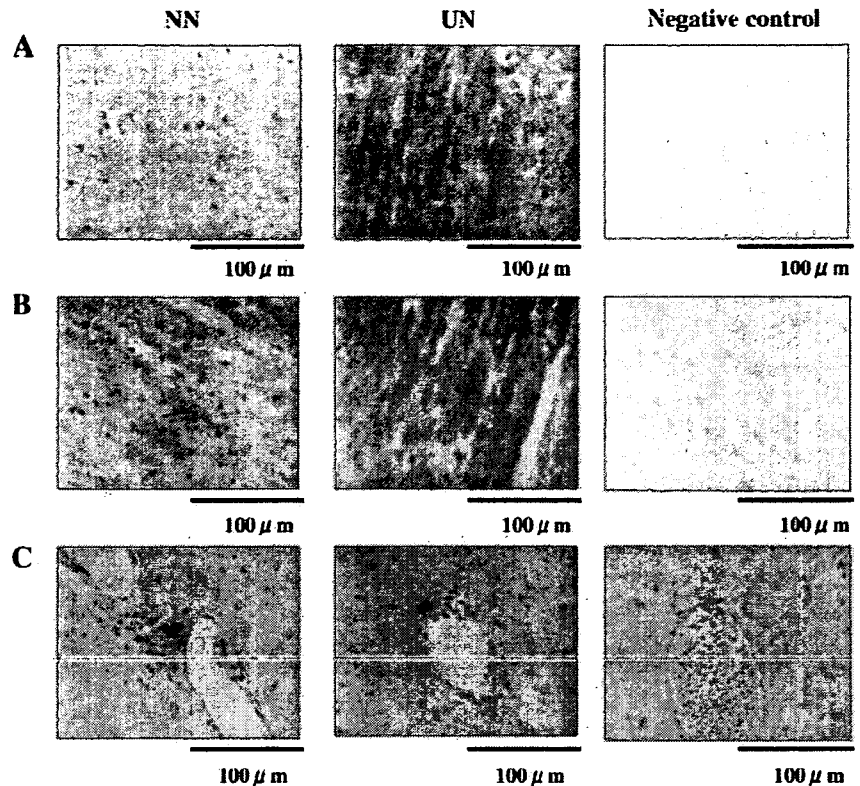
NN   UN   Negative control



FIG. 5. Immunohistochemistry for angiotensin II (A), ET-1 (B), and renin (C) in the left ventricles of NN offspring (*left panels*) and UN offspring (*middle panels*) at 16 wk. Negative controls of NN offspring using normal rabbit serum (for angiotensin II and ET-1) or goat serum for renin are shown in *right panels*. Original magnification was ×400.

Using the same animal model, we recently reported pronounced obesity in UN offspring on a high-fat diet compared with NN offspring (9). We found premature onset of the neonatal leptin surge, *i.e.* a transient increase in serum leptin levels during the neonatal period, in UN offspring. We also demonstrated that the premature leptin surge programs hypothalamic low sensitivity to circulating leptin, a potent anti-obesity hormone, causatively contributing to pronounced obesity on a high-fat diet in adulthood, by showing that an artificial premature leptin surge model produced hypothalamic low sensitivity to circulating leptin and pronounced obesity on a high-fat diet (9). However, in the present study, an artificial premature leptin surge did not increase SBP in NN offspring. Moreover, artificial premature leptin surge did not augment cardiac remodeling (Kawamura, M., and H. Itoh, unpublished observations). We also revealed that chemical injury of the ARC by neonatal monosodium glutamate treatment during the neonatal period cancelled the acceleration of obesity on the high-fat diet in UN offspring (9).

TABLE 4. The mRNA expression of Ang, AT1R, AT2R, ACE, ET-1, ANP, and BNP in the murine fetal whole heart at 18.5 dpc

|  | NN (n = 10) | UN (n = 10) |
|---|---|---|
| Ang/GAPDH | 0.38 ± 0.05 | 0.74 ± 0.17[a] |
| AT1R/GAPDH | 0.25 ± 0.02 | 0.31 ± 0.03 |
| AT2R/GAPDH | 4.88 ± 0.55 | 6.53 ± 1.11 |
| ACE/GAPDH | 0.10 ± 0.01 | 0.18 ± 0.03[b] |
| ET-1/GAPDH | 2.13 ± 0.22 | 3.22 ± 0.44[a] |
| ANP/GAPDH | 17.32 ± 1.93 | 22.58 ± 2.63 |
| BNP/GAPDH | 0.811 ± 0.07 | 0.70 ± 0.04 |

Values are the mean ± SEM (arbitrary units).
[a] $P < 0.05$; [b] $P < 0.01$ *vs.* NN offspring.

However, a significant increase in SBP was not blocked by monosodium glutamate treatment in the present study. The mechanisms leading to increased blood pressure in adult UN offspring with undernutrition *in utero* are currently not entirely clear.

There were no significant changes in the mRNA expression of cardiac RAS-associated bioactive substances at 3 wk (Figs. 3 and 4). On the other hand, at 8 wk, the mRNA expression of ET-1, a factor promoting cardiac remodeling (18, 19), was significantly elevated in the left ventricles of UN offspring (Fig. 4A). However, several anticardiac remodeling phenomena were observed at the same time in the left ventricles as follows. The Ang mRNA expression was significantly decreased (Fig. 3A), concomitantly with the significant increase of AT2R (Fig. 3D), which suppresses cardiac remodeling (20). ANP and BNP are secreted from the heart and antagonize RAS through a decrease in blood pressure, diuresis, anticardiac hypertrophy, and anticardiac fibrosis, *etc.* (21, 22). The significant elevation of BNP mRNA expression in the left ventricles of UN offspring at 8 wk, in parallel with a tendency for an increase in ANP mRNA expression, suggested protective effects on cardiac tissues against the acceleration of cardiac remodeling. Therefore, changes that both promote and suppress cardiac remodeling are simultaneously observed in the left ventricles of UN offspring at 8 wk. These findings lead us to speculate that a kind of compensatory mechanism might be operating, thereby protecting the heart from ominous cardiac transformation at 8 wk, which was relevant to the finding that neither cardiac hypertrophy (Table 3B) nor augmentation of perivascular

– 85 –

fibrosis (Fig. 2) was observed with a significant increase in SBP (Fig. 1).

At 16 wk, a significant augmentation of cardiac remodeling, *i.e.* cardiac hypertrophy (Table 3B) and perivascular fibrosis (Fig. 2), was observed in UN offspring. It is a further aim of the study to assess the movement and/or thickness of the ventricular wall by ultrasound examination.

In the present study, we first demonstrated that undernutrition *in utero* significantly increased the mRNA expression of both Ang (Fig. 3A) and ET-1 (Fig. 4A) in the left ventricles of UN offspring at 16 wk, concomitantly with the augmentation of cardiac hypertrophy and perivascular fibrosis. Angiotensin II is derived from Ang and plays a central role in the local cardiac RAS in the augmentation of cardiac remodeling (4, 5). ET-1 has been found to induce hypertrophy of cardiomyocytes (18), as well as cardiac fibrosis (19). ET-1 has a close association with the local cardiac RAS in the process of cardiac remodeling (23, 24). In the present study, the significant elevation of both Ang and ET-1 mRNA levels in the left ventricle of UN offspring was observed at 16 wk. The immunostaining of both angiotensin II and ET-1 showed a tendency to increase in UN offspring compared with NN offspring at 16 wk. These findings suggested a possible decompensation of cardiac homeostasis in response to various portentous factors, as a result of fetal undernutrition, including an increase in blood pressure. A significant elevation in the AT2R mRNA expression, which suppresses cardiac remodeling by antagonizing the effects of signaling through the AT1R (20), was observed in UN offspring at 8 and 16 wk, but the increase relative to NN offspring was much lower at 16 wk than at 8 wk (Fig. 3D). Long-term observations are necessary to prove that 16 wk is the beginning of decompensation of cardiac homeostasis in this animal model. Nevertheless, these findings suggested a possible involvement of local cardiac RAS activation in the developmental origins of cardiac remodeling.

Rather stable expression was observed in ACE and AT1R after birth in UN offspring. Ang mRNA expression decreased at 8 wk and increased at 16 wk. More detailed molecular investigation is necessary to clarify the regulatory mechanism of each substance.

A few renin positive cells were detected in the left ventricle at 16 wk (Fig. 5C), although mRNA expression was below detection sensitivity of quantitative RT-PCR. This discrepancy was relevant to the recent observation that cardiac renin was predominantly derived from circulation (25). There was no apparent difference in cardiac renin immunostaining between NN and UN offspring at 16 wk. It is an interesting study to investigate whether cardiac renin uptake is involved in developmental origins of cardiac remodeling.

A significant augmentation of mRNA expression of Ang, ACE, and ET-1 was observed in the whole fetal heart at 18.5 dpc (Table 4). A possible association of these changes with local cardiac RAS activation in adulthood is a future aim of the study.

In summary, using a mouse model of fetal undernutrition, we here demonstrated the possible involvement of the local cardiac RAS in the developmental origins of cardiac disorders, represented by cardiac remodeling, by a longitudinal assessment of the expression of local cardiac RAS-associated

bioactive substances from the fetal to adult periods. This study also highlighted the local cardiac RAS as a promising target for prophylactic intervention in the developmental origins of cardiovascular disease.

## References

1. Barker DJ, Gluckman PD, Godfrey KM, Harding JE, Owens JA, Robinson JS 1993 Fetal nutrition and cardiovascular disease in adult life. Lancet 341: 938–941
2. Gluckman PD, Hanson MA 2004 Living with the past: evolution, development, and patterns of disease. Science 305:1733–1736
3. Unger T 2003 Blood pressure lowering and renin-angiotensin system blockade. J Hypertens Suppl 21:S3–S7
4. Varagic J, Frohlich ED 2002 Local cardiac renin-angiotensin system: hypertension and cardiac failure. J Mol Cell Cardiol 34:1435–1442
5. Berecek KH, Reaves P, Raizada M 2005 Effects of early perturbation of the renin-angiotensin system on cardiovascular remodeling in spontaneously hypertensive rats. Vascul Pharmacol 42:93–98
6. Holemans K, Aerts L, Van Assche FA 2003 Fetal growth restriction and consequences for the offspring in animal models. J Soc Gynecol Investig 10: 392–399
7. Ozaki T, Nishina H, Hanson MA, Poston L 2001 Dietary restriction in pregnant rats causes gender-related hypertension and vascular dysfunction in offspring. J Physiol 530:141–152
8. Rasch R, Skriver E, Woods LL 2004 The role of the RAS in programming of adult hypertension. Acta Physiol Scand 181:537–542
9. Yura S, Itoh H, Sagawa N, Yamamoto H, Masuzaki H, Nakao K, Kawamura M, Takemura M, Kakui K, Ogawa Y, Fujii S 2005 Role of premature leptin surge in obesity resulting from intrauterine undernutrition. Cell Metab 1:371–378
10. Olney JW 1969 Brain lesions, obesity, and other disturbances in mice treated with monosodium glutamate. Science 164:719–721
11. Casellas D, Dupont M, Kaskel FJ, Inagami T, Moore LC 1993 Direct visualization of renin-cell distribution in preglomerular vascular trees dissected from rat kidney. Am J Physiol 265:F151–F156
12. Itoh H, Bird IM, Nakao K, Magness RR 1998 Pregnancy increases soluble and particulate guanylate cyclases and decreases the clearance receptor of natriuretic peptides in ovine uterine, but not systemic, arteries. Endocrinology 139:3329–3341
13. Lee G, Makhanova N, Caron K, Lopez ML, Gomez RA, Smithies O, Kim HS 2005 Homeostatic responses in the adrenal cortex to the absence of aldosterone in mice. Endocrinology 146:2650–2656
14. Lamireau D, Nuyt AM, Hou X, Bernier S, Beauchamp M, Gobeil Jr F, Lahaie I, Varma DR, Chemtob S 2002 Altered vascular function in fetal programming of hypertension. Stroke 33:2992–2998
15. Franco Mdo C, Arruda RM, Dantas AP, Kawamoto EM, Fortes ZB, Scavone C, Carvalho MH, Tostes RC, Nigro D 2002 Intrauterine undernutrition: ex-

pression and activity of the endothelial nitric oxide synthase in male and female adult offspring. Cardiovasc Res 56:145–153

16. **Woods LL, Ingelfinger JR, Nyengaard JR, Rasch R** 2001 Maternal protein restriction suppresses the newborn renin-angiotensin system and programs adult hypertension in rats. Pediatr Res 49:460–467

17. **Manalich R, Reyes L, Herrera M, Melendi C, Fundora I** 2000 Relationship between weight at birth and the number and size of renal glomeruli in humans: a histomorphometric study. Kidney Int 58:770–773

18. **Shubeita HE, McDonough PM, Harris AN, Knowlton KU, Glembotski CC, Brown JH, Chien KR** 1990 Endothelin induction of inositol phospholipid hydrolysis, sarcomere assembly, and cardiac gene expression in ventricular myocytes. A paracrine mechanism for myocardial cell hypertrophy. J Biol Chem 265:20555–20562

19. **Clozel M, Salloukh H** 2005 Role of endothelin in fibrosis and anti-fibrotic potential of bosentan. Ann Med 37:2–12

20. **Berk BC** 2003 Angiotensin type 2 receptor (AT2R): a challenging twin. Sci STKE 2003:PE16

21. **Itoh H, Nakao K** 1994 Antagonism between the vascular renin-angiotensin and natriuretic peptide systems in vascular remodelling. Blood Press Suppl 5:49–53

22. **Nakanishi M, Saito Y, Kishimoto I, Harada M, Kuwahara K, Takahashi N, Kawakami R, Nakagawa Y, Tanimoto K, Yasuno S, Usami S, Li Y, Adachi Y, Fukamizu A, Garbers DL, Nakao K** 2005 Role of natriuretic peptide receptor guanylyl cyclase-A in myocardial infarction evaluated using genetically engineered mice. Hypertension 46:441–447

23. **Yanagisawa M, Kurihara H, Kimura S, Tomobe Y, Kobayashi M, Mitsui Y, Yazaki Y, Goto K, Masaki T** 1988 A novel potent vasoconstrictor peptide produced by vascular endothelial cells. Nature 332:411–415

24. **Moreau P, d'Uscio LV, Shaw S, Takase H, Barton M, Luscher TF** 1997 Angiotensin II increases tissue endothelin and induces vascular hypertrophy: reversal by ET(A)-receptor antagonist. Circulation 96:1593–1597

25. **Peters J, Farrenkopf R, Clausmeyer S, Zimmer J, Kantachuvesiri S, Sharp MG, Mullins JJ** 2002 Functional significance of prorenin internalization in the rat heart. Circ Res 90:1135–1141

*Endocrinology* **is published monthly by The Endocrine Society (http://www.endo-society.org), the foremost professional society serving the endocrine community.**

# Role of MAPK Phosphatase-1 in the Induction of Monocyte Chemoattractant Protein-1 during the Course of Adipocyte Hypertrophy[*][S]

Ayaka Ito[‡§1], Takayoshi Suganami[‡], Yoshihiro Miyamoto[¶], Yasunao Yoshimasa[¶], Motohiro Takeya[‖],
Yasutomi Kamei[‡], and Yoshihiro Ogawa[‡§2]

From the ‡Department of Molecular Medicine and Metabolism and the §Center of Excellence Program for Frontier Research on Molecular Destruction and Reconstitution of Tooth and Bone, Medical Research Institute, Tokyo Medical and Dental University, 2-3-10 Kanda-surugadai, Chiyoda-ku, Tokyo 101-0062, Japan, the ¶Department of Medicine, Division of Atherosclerosis and Diabetes, National Cardiovascular Center Hospital, 5-7-1 Fujishirodai, Suita, Osaka 560-0005, Japan, and the ‖Department of Cell Pathology, Graduate School of Medical Sciences, Kumamoto University, 1-1-1 Honjo, Kumamoto 860-8556, Japan

Monocyte chemoattractant protein-1 (MCP-1), an important chemokine whose expression is increased during the course of obesity, plays a role in macrophage infiltration into obese adipose tissue. This study was designed to elucidate the role of mitogen-activated protein kinase (MAPK) phosphatase-1 (MKP-1) in the induction of MCP-1 during the course of adipocyte hypertrophy. We examined the time course of MKP-1 and MCP-1 mRNA expression and extracellular signal-regulated kinase (ERK) phosphorylation in the adipose tissue from mice rendered mildly obese by a short term high fat diet. We also studied the role of MKP-1 in the induction of MCP-1 in 3T3-L1 adipocytes during the course of adipocyte hypertrophy. MCP-1 mRNA expression was increased, followed by ERK activation and down-regulation of MKP-1, an inducible dual specificity phosphatase to inactivate ERK, in the adipose tissue at the early stage of obesity induced by a short term high fat diet, when macrophages are not infiltrated. Down-regulation of MKP-1 preceded ERK activation and increased production of MCP-1 in 3T3-L1 adipocytes in vitro during the course of adipocyte hypertrophy. Adenovirus-mediated restoration of MKP-1 in hypertrophied 3T3-L1 adipocytes reduced the otherwise increased ERK phosphorylation, thereby leading to the significant reduction of MCP-1 mRNA expression. This study provides evidence that the down-regulation of MKP-1 is critical for increased production of MCP-1 during the course of adipocyte hypertrophy.

Evidence has accumulated suggesting that obesity is a state of chronic, low grade inflammation; it may represent a potential mechanism whereby obesity leads to the metabolic derangements (1–3). Previous studies demonstrated that the adipose tissue is markedly infiltrated by macrophages in several models of rodent obesities and human obese subjects (4, 5). Using an *in vitro* co-culture system composed of adipocytes and macrophages, we have provided evidence that a paracrine loop involving saturated free fatty acids (FFAs) and tumor necrosis factor-α (TNFα) derived from adipocytes and macrophages, respectively, establishes a vicious cycle that aggravates the inflammatory changes; *i.e.* marked up-regulation of pro-inflammatory cytokines such as monocyte chemoattractant protein-1 (MCP-1)[3] and TNFα and down-regulation of anti-inflammatory adiponectin (6, 7). These findings have led us to speculate that macrophages, when infiltrated, may participate in the inflammatory pathways that are activated in obese adipose tissue.

A previous study with bone marrow transplantation demonstrated that most macrophages in the adipose tissue are derived from the bone marrow (4). In this regard, adipose tissue expression of MCP-1, a major chemokine implicated in the control of monocyte recruitment to the site of inflammation, is increased during the progression of obesity (8, 9) and is roughly correlated with macrophage markers in the adipose tissue (5, 10). These findings suggest that increased production of MCP-1 may be an initial event at the early stage of obesity so as to accumulate macrophages in the adipose tissue. Recently, Kanda *et al.* and Kamei *et al.* (11, 12) have independently reported that MCP-1 plays a role in the recruitment of macrophages into obese adipose tissue. It is, therefore, important to know the molecular mechanism for increased production of MCP-1 at the early stage of obesity. Recent studies have demonstrated that multiple intracellular signaling pathways are activated in adipocytes during the

- 88 -

course of adipocyte hypertrophy *in vitro* and in obese adipose tissue *in vivo*. However, how the inflammatory pathways are activated in adipocytes at the early stage of obesity is still poorly understood.

Mitogen-activated protein kinases (MAPKs) including extracellular signal-regulated kinase (ERK), p38 MAPK, and c-Jun $NH_2$-terminal kinase (JNK) are activated in a variety of cellular processes (13). Once activated by the upstream kinases, *e.g.* MAPK/ERK kinase (MEK), MAPKs are rapidly inactivated by a family of protein phosphatases such as MAPK phosphatase-1 (MKP-1), an inducible dual specificity phosphatase (14, 15). Sakaue *et al.* showed previously that MKP-1 plays an essential role in 3T3-L1 adipocyte differentiation through ERK down-regulation (16). On the other hand, Bost *et al.* (17) reported that mice lacking ERK1 (ERK1$^{-/-}$ mice) are protected from high fat diet-induced obesity and insulin resistance. These findings, taken together, suggest that the MAPK pathways play an important role in the adipocyte proliferation and differentiation *in vitro* and *in vivo* (18).

Here we show that MCP-1 mRNA expression is increased, which is followed by ERK activation and MKP-1 down-regulation in the adipose tissue from mice rendered mildly obese by a short term high fat diet, when macrophages are not infiltrated. We also demonstrate that ERK activation through MKP-1 down-regulation is involved in increased production of MCP-1 in 3T3-L1 adipocytes during the course of adipocyte hypertrophy. This study provides evidence that MKP-1 down-regulation is critical for the inflammatory changes in hypertrophied adipocytes at the early stage of obesity, thereby suggesting that MKP-1 activation may offer a novel therapeutic strategy to treat or reduce the inflammatory changes in adipocytes during the progression of obesity.

### EXPERIMENTAL PROCEDURES

*Materials*—Rabbit polyclonal antibodies against ERK, phospho-ERK, p38 MAPK, phospho-p38 MAPK, MEK1/2, phospho-MEK1/2, MEK inhibitors PD98059 and U0126, and a p38MAPK inhibitor SB203580 were purchased from Cell Signaling (Beverly, MA). Rabbit polyclonal antibodies against JNK, phospho-JNK, and MKP-1 and a mouse monoclonal antibody against Lamin A/C were purchased from Santa Cruz Biotechnology (Santa Cruz, CA). All other reagents were purchased from Sigma or Nacalai Tesque (Kyoto, Japan).

*Animal Studies*—Four-week-old male C57BL/6J mice were purchased from Charles River Laboratories Japan (Tokyo, Japan). The animals were housed in a temperature-, humidity-, and light- controlled room (12-h light and 12-h dark cycle) and allowed free access to water and chow. Five-week-old mice were fed either the standard chow (Oriental MF, 362 kcal/100 g, 5.4% energy as fat; Oriental Yeast, Tokyo, Japan) or high fat diet (D12492, 524 kcal/100 g, 60% energy as fat; Research Diets, New Brunswick, NJ) for 15 weeks. They were fasted for 1 h (12:00 –13:00) and sacrificed to harvest the epididymal adipose tissue before ($n$ = 10) and 2 weeks ($n$ = 10), 4 weeks ($n$ = 12), 6 weeks ($n$ = 11), 8 weeks ($n$ = 6), and 15 weeks ($n$ = 4) after the experiments. All animal experiments were conducted according to the guide-

lines of Tokyo Medical and Dental University Committee on Animal Research (No. 0060026).

*Histological Analysis*—The epididymal WAT was fixed with neutral-buffered formalin and embedded in paraffin. Sections were stained with hematoxylin and eosin and studied under ×200 magnification to measure the adipocyte area using Win Roof software (Mitani Corporation, Tokyo, Japan) (19). Immunohistochemical study was carried out using 5-$\mu$m thick paraffin-embedded sections for macrophage marker F4/80 as previously described (20, 21).

*Cell Culture*—3T3-L1 preadipocytes (American Type Culture Collection, Manassas, VA) were maintained as described (6, 7). Differentiation of 3T3-L1 preadipocytes to adipocytes was described elsewhere (6, 7). Cells at day 8 and day 21 after the induction of differentiation were used as non-hypertrophied and hypertrophied adipocytes, respectively (6). Accumulation of triglyceride in adipocytes was detected by oil red O staining (19).

*Measurement of Triglyceride Content*—Triglyceride content in 3T3-L1 adipocytes was measured as previously reported (22). In brief, 3T3-L1 adipocytes in 35-mm dish were harvested, and cellular lipid was extracted by chloroform-methanol (2:1). After evaporation, precipitation was dissolved in isopropyl alcohol. Triglyceride content was measured using a colorimetric assay kit (triglyceride E-test Wako, Wako Pure Chemicals, Osaka, Japan) according to the manufacturer's instructions.

*Quantitative Real-time PCR*—Quantitative real-time PCR was performed with an ABI Prism 7000 Sequence Detection System using PCR Master Mix reagent kit (Applied Biosystems, Foster City, CA) as described (6, 19). Primers used were described in supplemental Table S1. Levels of mRNAs were normalized to those of housekeeping gene 36B4 mRNA.

*ELISA*—The MCP-1, IL-6, and adiponectin levels in culture supernatants were determined by the commercially available ELISA kits (MCP-1 and IL-6, R&D systems, Minneapolis, MN; adiponectin, Otsuka Pharmaceutical, Tokyo, Japan).

*Immunoblot Assay*—Nuclear and cytosolic extracts were prepared by using the Nuclear/Cytosol fractionation kit (Bio-Vision, Mountain View, CA). Separation of nuclear and cytosolic proteins was confirmed by immunoblots with $\alpha$-tubulin and lamin A/C antibodies, respectively. Whole cell lysates were prepared using buffer containing 50 mmol/liter HEPES (pH7.5), 150 mmol/liter NaCl, 100 mmol/liter sodium fluoride, 1 mmol/liter EGTA, 1 mmol/liter EDTA, 1% Triton X-100, 2 mmol/liter sodium vanadate, 2 mmol/liter phenylmethylsulfonyl fluoride, and protease inhibitor mixture (Sigma). Immunoblot assay was performed as described (6). Samples (10 –20 $\mu$g protein/lane) were separated by 12.5% SDS-PAGE and electrophoretically transferred onto polyvinylidene difluoride filter membrane (PolyScreen; PerkinElmer, Wellesley, MA). After membranes were incubated with primary antibodies for 1 h at room temperature, immunoblots were developed with horseradish peroxidase-conjugated secondary antibodies (GE Healthcare Bio-Sciences, Piscataway, NJ) and a chemiluminescence kit (GE Healthcare Bio-Sciences). The signals were detected with LAS3000 (Fuji Photo Film, Tokyo, Japan).

- 89 -

*Generation of 3T3-L1 Adipocytes Stably Expressing Cox-sackie-Adenovirus Receptor (CAR)*—A mouse CAR-expressing plasmid pcDNA3-CAR (23) was kindly provided by Dr. Hiroyuki Mizuguchi (National Institute of Biomedical Innovation, Osaka, Japan). The CAR retroviral expression vector (pMRX-CAR) was constructed by ligating the full-length CAR cDNA into the EcoR1 site of pMRX vector (24) and transfected into Plat-E packaging cells (25) using Lipofectamine2000 (Invitrogen) according to the manufacturer's instructions. Viral supernatants were harvested from 24 to 48 h after transfection and applied to 3T3-L1 adipocytes in Dulbecco's modified Eagle's medium containing 10% fetal bovine serum and 5 $\mu$g/ml of polybrene (Nacalai Tesque) in a final volume of 5 ml. The stable CAR-expressing 3T3-L1 adipocytes (CAR-3T3-L1 adipocytes) were obtained by 2 $\mu$g/ml of puromycin (Nacalai Tesque) selection.

*Adenovirus-mediated Expression of MKP-1*—The adenoviral vector expressing mouse MKP-1 (Ad-MKP-1) (26), kindly provided by Dr. Jeffery D. Molkentin (University of Cincinnati, Cincinnati, OH), was prepared using HEK293 cells and purified by VIRAPREP adenovirus purification kit (Virapur, LLC, San Diego, CA) as previously described (27). The GFP adenovirus (Ad-GFP; Clontech Laboratories, Palo Alto, CA) was used as a control. The CAR-3T3-L1 adipocytes at day 5 and day 18 after the induction of differentiation were transfected with Ad-MKP-1, incubated for 3 days, and harvested to be used for quantitative real-time PCR and immunoblot assay.

*Statistical Analysis*—Data are shown as means ± S.E. Statistical analysis was performed using the Student's $t$ test and analysis of variance followed by Scheffe's test. $p < 0.05$ was considered statistically significant.

## RESULTS

*MCP-1 mRNA Expression in the Adipose Tissue from Mice with Diet-induced Obesity*—Body weight was increased significantly in mice fed high fat diet for 2 weeks relative to those fed standard diet ($p < 0.01$) (Fig. 1A). The mice fed high fat diet weighed ~20% more than those fed standard diet for 15 weeks (29.7 ± 0.3 g versus 34.8 ± 1.9 g, $p < 0.05$). The weight of epididymal white adipose tissue (WAT) was significantly increased in mice fed high-fat diet for 2 weeks relative to those fed standard diet (0.26 ± 0.01 g versus 0.49 ± 0.04 g, $p < 0.01$). Histological examination revealed appreciable increase in adipocyte cell size in mice fed a high fat diet during the initial 2 weeks, which reached up to ~4-fold larger than that in mice fed standard diet after 15 weeks (Fig. 1B). There were no appreciable infiltration of macrophages in the adipose tissue up to 8 weeks after the experiment, after which interstitial cells stained with F4/80, a marker of activated macrophages, appeared in mice fed high fat diet (Fig. 1C). Correspondingly, F4/80 mRNA expression was also increased in the epididymal WAT in mice fed high fat diet for 15 weeks relative to those fed standard diet (Fig. 1D, left). In mice fed high fat diet, MCP-1 mRNA expression was increased as early as 4 weeks and gradually increased up to 15 weeks after the experiment (Fig. 1D, right). These observations indicate that MCP-1 mRNA expression is increased prior to macrophage infiltration at the early stage of obesity.
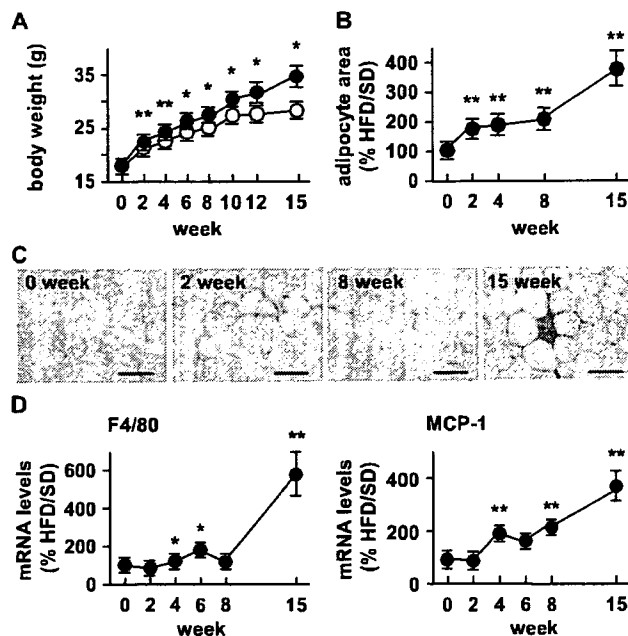


FIGURE 1. **Time course of adipocyte hypertrophy and macrophage infiltration in mice with diet-induced obesity.** Five-week-old male C57BL/6J mice were fed either SD or HFD for 15 weeks. A, time course of body weight. Open circle, SD; closed circle, HFD. B, time course of adipocyte area. C, macrophage marker F4/80 immunostaining of the epididymal WAT in diet-induced obese mice. Original magnification, ×200. Scale bars, 100 $\mu$m. D, time courses of F4/80 and MCP-1 mRNA expression. Data in B and D are expressed as the ratio of changes in mice fed HFD to those in mice fed SD. *, $p < 0.05$; **, $p < 0.01$ versus SD, $n = 4$–12 at each time point.

*Dysregulation of Adipocytokine Production during the Course of Adipocyte Hypertrophy*—To explore the molecular mechanisms underlying adipocyte hypertrophy, we cultured 3T3-L1 adipocytes up to 21 days after the induction of differentiation; they exhibited a gradual increase in lipid accumulation from day 8 to day 21 during the course of adipocyte hypertrophy as revealed by oil-red O staining (Fig. 2A) and triglyceride content (Fig. 2B). In this study, insulin-induced glucose uptake was preserved up to day 21 (supplemental Fig. S1).

Quantitative real-time PCR analysis revealed that MCP-1 mRNA expression was significantly increased up to day 21, ~6-fold higher than that in 3T3-L1 adipocytes (day 8) ($p < 0.01$), in parallel with increased cell size and lipid accumulation (Fig. 2C). Expression of IL-6 mRNA was also increased during the course of adipocyte hypertrophy. The IL-6 mRNA levels in 3T3-L1 adipocytes (day 21) were ~5-fold higher than those in 3T3-L1 adipocytes (day 8) ($p < 0.01$). By contrast, adiponectin mRNA expression showed significant reduction (up to 30%) during the course of adipocyte hypertrophy ($p < 0.01$). The MCP-1, IL-6, and adiponectin concentrations in the culture media were roughly parallel to their respective mRNA levels (Fig. 2D). The expression patterns of adipocytokines in hypertrophied 3T3-L1 adipocytes (day 21) were similar to those found in obese adipose tissue. We also confirmed that mRNA expression patterns of adipogenesis-related markers such as peroxisome proliferator-activated receptor $\gamma$2 (PPAR$\gamma$2), adipocyte fatty acid-binding protein (aP2), fatty-acid transport protein 1 (FATP1), and CCAAT/enhancer-binding protein $\alpha$
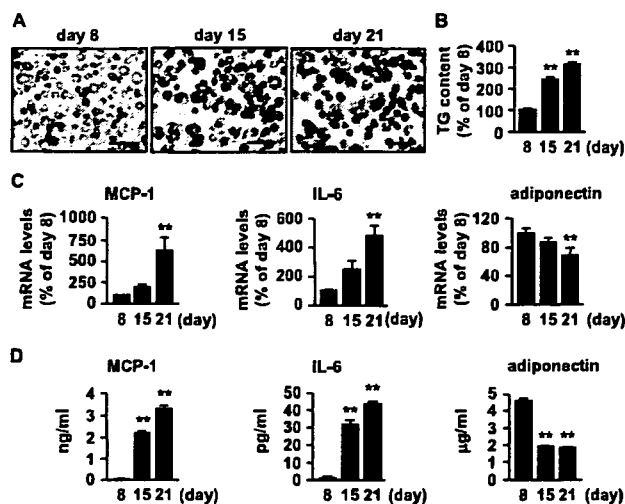
- 90 -

FIGURE 2. **Changes in adipocytokine expression during the course of adipocyte hypertrophy** *in vitro.* *A,* morphological changes of 3T3-L1 adipocytes during the course of adipocyte hypertrophy (day 8-day 21) as revealed by oil-red O staining. Original magnification, ×200. *Scale bars,* 100 μm. *B,* triglyceride accumulation in 3T3-L1 adipocytes during the course of adipocyte hypertrophy. *C* and *D,* changes in adipocytokine mRNA expression (*C*) and secretion (*D*) in 3T3-L1 adipocytes during the course of adipocyte hypertrophy. **, $p < 0.01$ versus day 8. $n = 4$.



FIGURE 3. **Role of MAP kinases in MCP-1 mRNA expression in hypertrophied adipocytes.** *A,* phosphorylation of MAP kinases during the course of adipocyte hypertrophy. Representative immunoblots of ERK, p38 MAPK and JNK quantification of phosphorylation levels. *, $p < 0.05$; **, $p < 0.01$ versus day 8. $n = 4$. *B,* effect of 24-h-treatment with MAP kinase inhibitors on MCP-1 mRNA expression (*left*) and secretion (*right*) in hypertrophied 3T3-L1 adipocytes (day 21). *PD,* PD98059, 20 μmol/liter; *U,* U0126, 10 μmol/liter; *SB,* SB203580, 10 μmol/liter. **, $p < 0.01$ versus vehicle treated day 21. $n = 6$. *N.S.,* not significant. *C,* effect of 6-h-treatment with MAPK inhibitors on MCP-1 mRNA expression in hypertrophied 3T3-L1 adipocytes (day 21). *D,* phosphorylation of ERK in the cytosolic and nuclear fractions from non-hypertrophied (day 8) and hypertrophied (day 21) 3T3-L1 adipocytes. Representative immunoblots of ERK and quantification of phosphorylation levels. *E,* phosphorylation of MEK during the course of adipocyte hypertrophy. Representative immunoblots of MEK and quantification of phosphorylation levels. **, $p < 0.01$ versus day 8. $n = 4-6$.

(C/EBPα) in hypertrophied 3T3-L1 adipocytes were consistent with those in obese adipose tissue (supplemental Fig. S2). In this study, we used 3T3-L1 adipocytes cultured for 8 and 21 days after differentiation as non-hypertrophied (day 8) and hypertrophied (day 21) adipocytes, respectively.

*Activation of MAPK Pathways during the Course of Adipocyte Hypertrophy*—To explore the role of MAPK activation in the dysregulation of MCP-1 production during the course of adipocyte hypertrophy, we examined phosphorylation of ERK, p38 MAPK, and JNK in 3T3-L1 adipocytes during the course of adipocyte hypertrophy. Immunoblot analysis revealed that phosphorylation of ERK and p38 MAPK is increased in hypertrophied adipocytes relative to non-hypertrophied adipocytes (Fig. 3A). In this study, there was no significant induction of phosphorylation of JNK during the course of adipocyte hypertrophy (Fig. 3A). Treatment of hypertrophied adipocytes with MEK inhibitors, PD98059 and U0126, for 24 h significantly reduced MCP-1 mRNA levels (Fig. 3B left, $p < 0.01$) and secretion in the culture media (Fig. 3B right, $p < 0.01$). Moreover, the effect of the MEK inhibitors on MCP-1 mRNA expression was observed as early as 6 h after the treatment (Fig. 3C). Furthermore, phosphorylation of ERK was increased in the nuclear fraction rather than in the cytosolic fraction from hypertrophied adipocytes (Fig. 3D, $p < 0.01$). We also confirmed that phosphorylation of MEK is increased in hypertrophied adipocytes (Fig. 3E, $p < 0.01$). On the other hand, no such inhibitory effect was observed when treated with a p38 MAPK inhibitor, SB203580 (Fig. 3, *B* and *C*). These observations suggest that increased mRNA expression and secretion of MCP-1 in hypertrophied adipocytes are due at least in part to MEK-ERK activation.

*MKP-1 Down-regulation during the Course of Adipocyte Hypertrophy*—We next examined expression of members of the MKP family during the course of adipocyte hypertrophy.
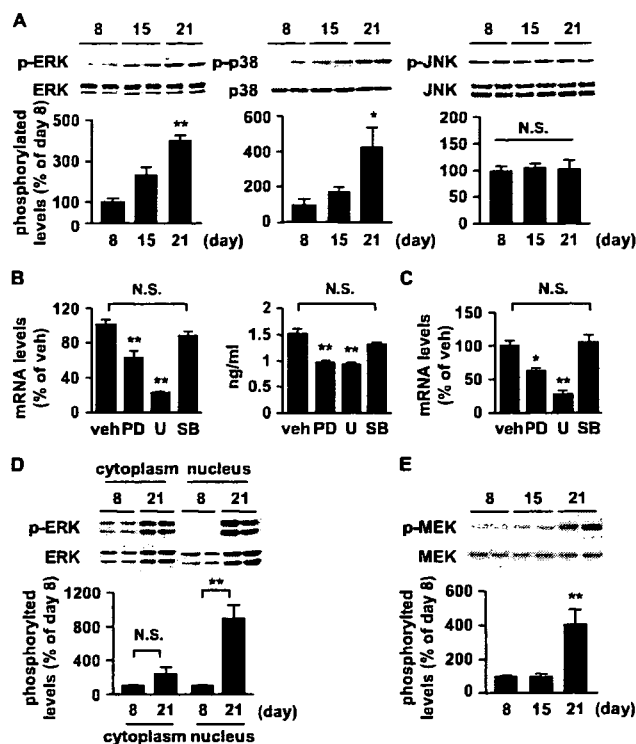
Interestingly, we detected substantial amounts of MKP-1 mRNA and protein in non-hypertrophied adipocytes, which are markedly down-regulated in hypertrophied adipocytes (Fig. 4, *A* and *B*, $p < 0.05$). There were no obvious changes in MKP-2 and MKP-3 mRNA levels during the course of adipocyte hypertrophy (Fig. 4A). We also observed that MKP-1 mRNA expression is significantly down-regulated in the adipose tissue from mice fed high fat diet for 2- and 4-weeks relative to those fed standard diet (Fig. 4C, $p < 0.05$). In addition, phosphorylation of ERK was significantly increased in the adipose tissue from mice that received 4-, 6-, 8-, and 15-week high fat diet relative to those fed standard diet (Fig. 4D, $p < 0.05$). These observations, taken together, suggest that MKP-1 is down-regulated in hypertrophied adipocytes, which is accompanied by ERK activation *in vivo.*

*Generation of CAR-3T3-L1 Adipocytes*—Because MKP-1 down-regulation may be responsible for the induction of MCP-1 during the course of adipocyte hypertrophy, we next examined the effect of MKP-1 restoration on ERK activity and
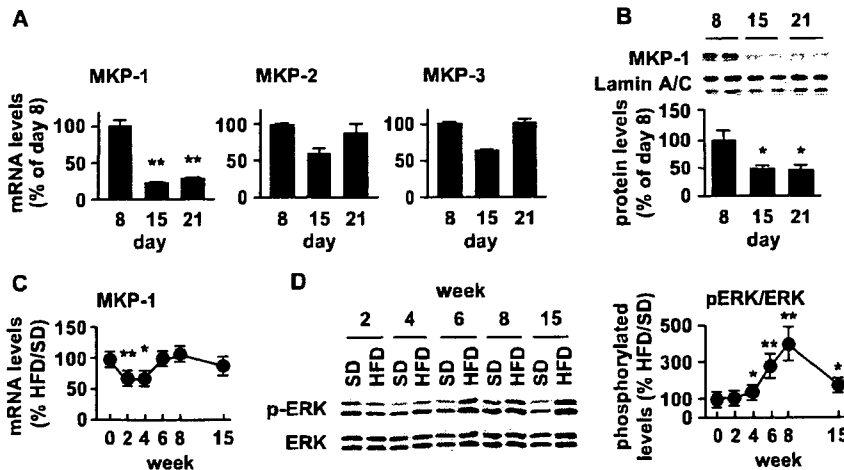
- 91 -

**A**



**B**



**C**

**D**



FIGURE 4. **Changes in MKP-1 expression during the course of adipocyte hypertrophy** *in vitro* **and** *in vivo*. *A*, changes in mRNA expression of MKP family during the course of adipocyte hypertrophy. *n* = 6. *B*, changes in MKP-1 protein levels in 3T3-L1 adipocytes during the course of adipocyte hypertrophy. Representative immunoblots of MKP-1 and quantification of protein levels. *n* = 4. *, *p* < 0.05; **, *p* < 0.01 *versus* day 8. *C* and *D*, time course of MKP-1 mRNA expression (*C*) and ERK phosphorylation (*D*) levels in mice with diet-induced obesity. Representative immunoblots of ERK and quantification of phosphorylation levels. Data in *C* and *D* are expressed as the ratio of changes in mice fed HFD to those in mice fed SD. *, *p* < 0.05; **, *p* < 0.01 *versus* SD. *n* = 4–12 at each time point.

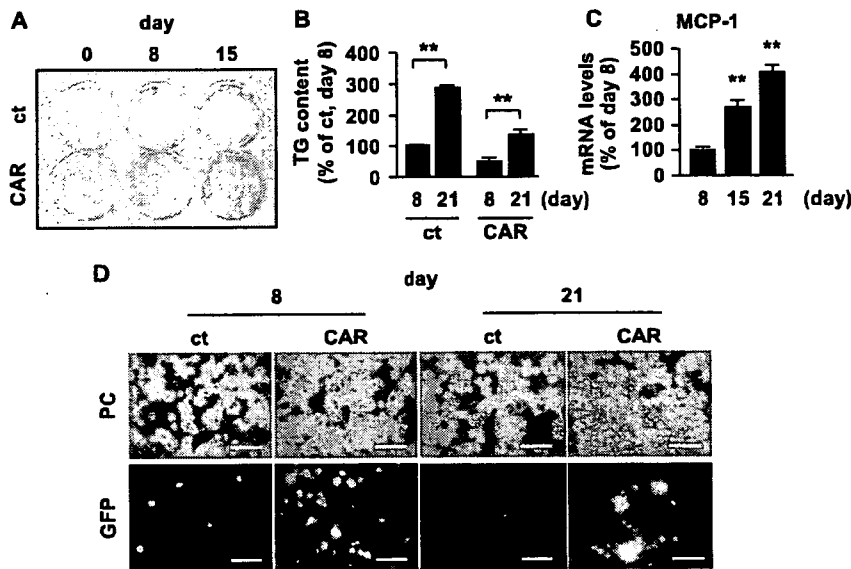**A**

**B**

**C**

**D**



FIGURE 5. **Generation of 3T3-L1 adipocytes stably expressing CAR (CAR-3T3-L1 adipocytes).** *A* and *B*, lipid accumulation of CAR-3T3-L1 adipocytes and control 3T3-L1 adipocytes (*ct*) during the course of adipocyte differentiation and hypertrophy as revealed by oil-red O staining (*A*) and triglyceride content (*B*). *C*, changes in MCP-1 mRNA expression in CAR-3T3-L1 adipocytes. *D*, efficiency of adenovirus-mediated gene transfer in CAR-3T3-L1 adipocytes using Ad-GFP. *PC*, phase contrast view; *GFP*, GFP fluorescence view. Original magnification, ×200. *Scale bars*, 100 μm. **, *p* < 0.01 *versus* day 8. *n* = 4.

MCP-1 mRNA expression in hypertrophied adipocytes. Because hypertrophied 3T3-L1 adipocytes are difficult to transfect with plasmid- or even virally encoded genes, we generated CAR-3T3-L1 adipocytes as described under "Experimental Procedures." There was no obvious difference in lipid accumulation between CAR-3T3-L1 and 3T3-L1 adipocytes without retroviral infection (control 3T3-L1 adipocytes) (Fig. 5, *A* and *B*) during the course of adipocyte differentiation and hypertrophy. We also confirmed no appreciable difference in mRNA expression of adipogenesis-related markers and adipocytokines

between the cells (supplemental Fig. S3). Similar to control 3T3-L1 adipocytes, CAR-3T3-L1 adipocytes exhibited the up-regulation of MCP-1 during the course of adipocyte hypertrophy (Fig. 5C). The transfection efficiency was markedly increased in CAR-3T3-L1 adipocytes relative to control 3T3-L1 adipocytes as judged by Ad-GFP infection (Fig. 5D).

*Effect of MKP-1 Restoration in Hypertrophied Adipocytes*—Infection with Ad-MKP-1 significantly increased MKP-1 mRNA expression in hypertrophied CAR-3T3-L1 adipocytes (Fig. 6A, *left*). We confirmed that MKP-1 protein levels in hypertrophied CAR-3T3-L1 adipocytes infected with Ad-MKP-1 are roughly comparable to those found in non-hypertrophied CAR-3T3-L1 adipocytes (Fig. 6A, *right*). In this setting, MKP-1 restoration in hypertrophied CAR-3T3-L1 adipocytes resulted in a marked reduction of ERK phosphorylation (Fig. 6B, *p* < 0.05) and MCP-1 mRNA expression (Fig. 6C, *p* < 0.01), which is roughly comparable to those found in non-hypertrophied CAR-3T3-L1 adipocytes. Interestingly, adiponectin mRNA expression was significantly increased and IL-6 mRNA expression tended to be reduced in hypertrophied CAR-3T3-L1 adipocytes with Ad-MKP-1 infection (supplemental Fig. S4), suggesting the anti-inflammatory effect of MKP-1 in hypertrophied adipocytes. Of note, there was no obvious difference in mRNA expression of adipogenesis-related markers by Ad-MKP-1 infection (supplemental Fig. S4). We also confirmed that Ad-MKP-1 infection does not

affect lipid accumulation and insulin-induced glucose uptake in hypertrophied CAR-3T3-L1 (supplemental Fig. S5). These observations, taken together, indicate that restoration of MKP-1 does not affect adipocyte differentiation and hypertrophy but improves the overall inflammatory changes in hypertrophied adipocytes.

## DISCUSSION

Recent studies showed that obese adipose tissue is characterized by increased infiltration of macrophages, suggesting that
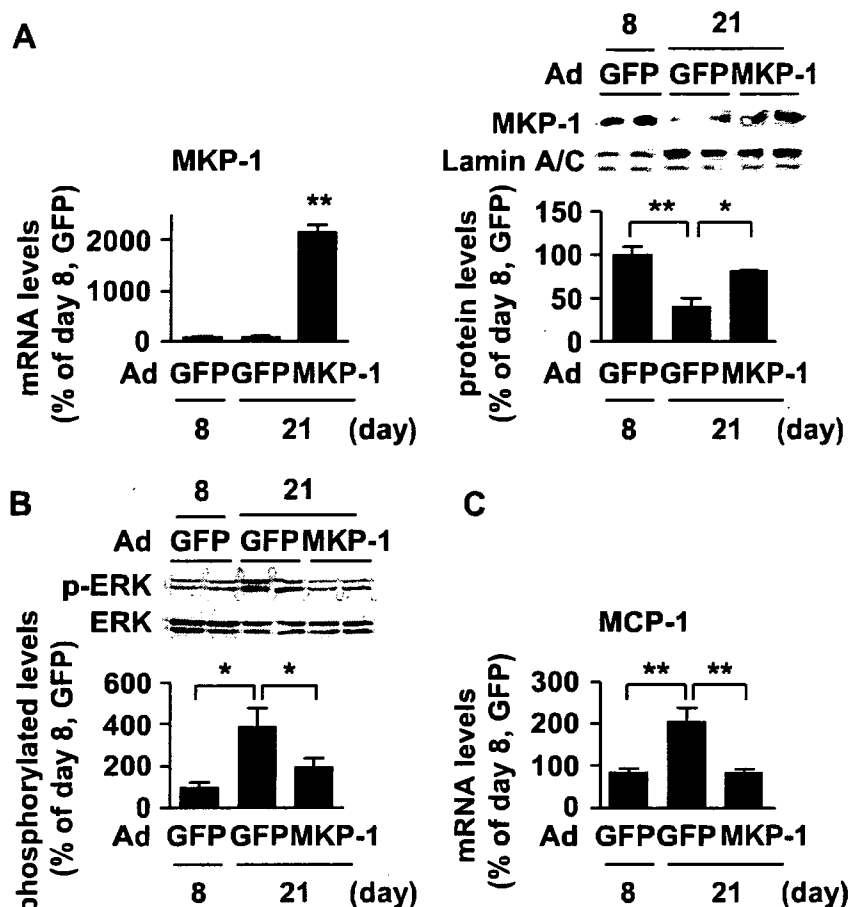
– 92 –

FIGURE 6. **Effect of MKP-1 restoration on ERK phosphorylation and MCP-1 mRNA expression in hyper-trophied adipocytes.** A, adenovirus-mediated restoration of MKP-1 in hypertrophied CAR-3T3-L1 adipocytes (day 21). Changes in MKP-1 mRNA (left) and protein (right) expression. Representative immunoblots of MKP-1 and quantification of protein levels. B and C, effect of MKP-1 restoration on ERK phosphorylation (B) and MCP-1 mRNA expression (C). *, $p < 0.05$; **, $p < 0.01$ versus Ad-GFP, (day 21). $n = 6$.

Weisberg et al. (28) reported the attenuation of macrophage content and inflammatory changes in the adipose tissue from mice lacking C-C motif chemokine receptor-2, a major receptor for MCP-1, during a long term high fat diet. Together with recent evidence that MCP-1 mRNA expression and secretion in primary cultured adipocytes from obese subjects are positively correlated with their cell size (29), our data herein support the concept that increased production of MCP-1 in hypertrophied adipocytes at the early stage of obesity contributes to increased infiltration of macrophages into the adipose tissue at the late stage of obesity.

There are multiple intracellular signaling pathways activated in adipocytes during the course of adipocyte hypertrophy. The data of this study demonstrate that 3T3-L1 adipocytes, when cultured alone up to 21 days after differentiation, is capable of up-regulating MCP-1 and IL-6 and down-regulating adiponectin in parallel with increased cell size and lipid accumulation, which are comparable to those in obese adipose tissue. Moreover, mRNA expression patterns of some adipogenesis-related markers are also roughly parallel to those in obese adipose tissue, suggesting that 3T3-L1 adipocytes cultured from day 8 to day 21 serve as the useful in vitro experimental model system to investigate the molecular mechanism for the dysregulation of adipocytokine production during the course of adipocyte hypertrophy.

the inflammatory changes induced by the cross-talk between adipocytes and macrophages are critical for the pathophysiology of obesity and thus the metabolic syndrome (4, 5). The molecular mechanisms underlying the recruitment of macrophages into obese adipose tissue have not fully been elucidated, but there is considerable evidence suggesting the involvement of MCP-1, which is increased during the course of obesity (8, 9). It is, therefore, important to know how MCP-1 is increased in hypertrophied adipocytes at the early stage of obesity, when macrophages are not infiltrated. This study was designed to elucidate the signaling pathway that mediates increased production of MCP-1 at the early stage of obesity.

In this study, we found that expression of MCP-1 mRNA is increased in the adipose tissue from mice rendered mildly obese by a short term high fat diet. Histologically, there is marked increase in adipocyte cell size with no obvious macrophage infiltration, suggesting that MCP-1 mRNA expression is increased in the adipose tissue prior to macrophage accumulation in vivo. Two recent studies with transgenic mice overexpressing MCP-1 in the adipose tissue and/or MCP-1-deficient mice showed that MCP-1 plays a role in the recruitment of macrophages into obese adipose tissue (11, 12). Furthermore,

In this study, we observed that ERK and p38 MAPK are activated in hypertrophied 3T3-L1 adipocytes. Moreover, increased production of MCP-1 is significantly suppressed by MEK inhibitors as early as 6 h after the treatment, but not by a p38 MAPK inhibitor. We also demonstrated that ERK phosphorylation is significantly increased in the nuclear fraction but not in cytosolic fraction obtained from non-hypertrophied (day 8) and hypertrophied (day 21) 3T3-L1 adipocytes, suggesting that ERK activation occurs mostly in the nucleus rather than in the cytoplasm of adipocytes during the course of adipocyte hypertrophy. These observations are consistent with the concept that MKP-1 acts as a negative regulator of MAPKs within the nucleus (30). Furthermore, we observed that phosphorylation of MEK is increased in hypertrophied adipocytes. Together with a recent report that MAPKs are involved in the regulation of MCP-1 in human adipose tissue (31), these observations suggest that increased production of MCP-1 in hypertrophied adipocytes is mediated at least in part thorough MEK-ERK activa-

- 93 -

tion. In this regard, using the TRANSFAC (6.0) data base, we also searched for transcriptional factor binding sites in the mouse, rat, and human MCP-1 promoter and found a consensus AP-1 binding site 3–4-kb upstream of the transcriptional start site. Moreover, there are previous reports showing that cytokine-induced MCP-1 is mediated at least in part through the activation of ERK and AP-1 (32, 33). It is, therefore, conceivable that decrease in MKP-1 leads to the activation of ERK and AP-1 transcriptional activity within the nucleus, thereby increasing MCP-1 production during the course of adipocyte hypertrophy.

In this study, we demonstrate for the first time that both MKP-1 mRNA and protein levels are significantly down-regulated during the course of adipocyte hypertrophy *in vitro*. Moreover, restoration of MKP-1 in hypertrophied adipocytes reduces the otherwise increased ERK phosphorylation and thus MCP-1 mRNA expression. These observations, taken together, suggest that ERK activation through MKP-1 down-regulation is involved in increased production of MCP-1 in 3T3-L1 adipocytes during the course of adipocyte hypertrophy. The above discussion is consistent with the *in vivo* observation that ERK is activated, which is followed by MKP-1 down-regulation in the adipose tissue at the early stage of obesity, when there is no appreciable macrophage infiltration. Thus, reduced MKP-1 expression may be one of the early events during the progression of obesity *in vivo*, thereby leading to increased production of MCP-1 through the activation of ERK. In this regard, constitutive activation of ERK as a result of low induction of MKP-1 confers stronger resistance of immortalized cells than that of normal human fibroblasts to a cancer therapy called photodynamic therapy (34, 35). It is also noteworthy that MKP-1 expression is down-regulated in human ovarian cancer cell lines, where its forced re-expression reduces their malignant potential, suggesting the role of MKP-1 in the progression of human ovarian cancer (36). Thus, imbalance between MKP-1 and MEK activities as a result of MKP-1 down-regulation may cause ERK activation, thereby leading to increased production of MCP-1 in hypertrophied adipocytes.

It is also important to know the upstream signaling pathways responsible for MKP-1 down-regulation during the course of adipocyte hypertrophy. Recent studies have suggested the involvement of multiple intracellular signaling pathways in the inflammatory changes in adipocytes *in vitro* and in obese adipose tissue *in vivo*. For instance, Özcan *et al.* (37) reported that obesity is associated with the induction of ER stress predominantly in the adipose tissue and liver and demonstrated that ER stress is a central feature of obesity-related insulin resistance and type 2 diabetes. On the other hand, Furukawa *et al.* showed that ROS production is increased in parallel with lipid accumulation in 3T3-L1 adipocytes and that oxidative stress induces the dysregulation of adipocytokine production (38). It is, therefore, interesting to investigate the relationship among ER stress induction, ROS production, and MKP-1 activation during the course of adipocyte hypertrophy and/or at the early stage of obesity. Lin *et al.* (39, 40) demonstrated previously that MKP-1 degradation via the ubiquitin-proteasome pathway is stimulated by ERK, thereby leading to the sustained activation of

ERK. Whether MKP-1 is thus down-regulated in hypertrophied adipocytes or not must await further investigations.

During the course of this study, Wu *et al.* (41) have reported that mice deficient in MKP-1 (MKP-1$^{-/-}$ mice) exhibit enhanced MAPK activity in the adipose tissue, reduced adipocyte cell size relative to wild-type littermates, and resistance to diet-induced obesity as a result of increased lipid metabolism in the liver and oxygen consumption in the skeletal muscle. Using mice with congenital deficiency of MKP-1, however, the authors did not address the role of MKP-1 in adipocytes during the course of adipocyte hypertrophy or at the early stage of obesity. In this regard, Bost *et al.* (17) reported that ERK1$^{-/-}$ mice have decreased adiposity and fewer adipocytes than wild-type littermates, and are resistant to high fat diet-induced obesity and insulin resistance. In this study, we demonstrated that ERK activation through the down-regulation of MKP-1 plays a role in increased production of MCP-1 in hypertrophied adipocytes during the course of obesity. It is, therefore, tempting to speculate that ERK activation through the down-regulation of MKP-1 plays an important role in the regulation of adipocyte differentiation, adiposity, and high fat diet-induced obesity *in vivo*. In this study, we also found that restoration of MKP-1 improves the dysregulation of adipocytokine production in hypertrophied adipocytes, which may improve obesity-related insulin resistance via adipocytokine mechanism *in vivo*. The pathophysiologic role of MKP-1 down-regulation in hypertrophied adipocytes at the early stage of obesity *in vivo* must await further investigation.

To obtain hypertrophied 3T3-L1 adipocytes whose MKP-1 levels are restored to those of non-hypertrophied 3T3-L1, we tried to produce 3T3-L1 adipocytes stably expressing MKP-1 using the retrovirus vector and observed that they are unable to differentiate into lipid-laden mature adipocytes.[4] This is consistent with the concept that ERK should be on and off properly during adipogenesis *in vitro* (16, 42). Although the adenoviral vector has been widely used for the introduction of exogenous genes in non-proliferating cells, 3T3-L1 adipocytes, particularly when hypertrophied, are transfected with less efficiency because of the scarcity of CAR (43–45). In this study, we generated 3T3-L1 adipocytes stably expressing CAR (or CAR-3T3-L1 adipocytes), which is infected with the adenoviral expression vector with ease, even after being hypertrophied. Importantly, there are no appreciable differences in adipogenesis, lipid accumulation, and adipocytokine expression during the course of adipocyte differentiation and hypertrophy between CAR-3T3-L1 adipocytes and control 3T3-L1 adipocytes. This study has verified the usefulness of CAR-3T3-L1 adipocytes as the unique experimental tool to investigate the molecular basis for adipocyte differentiation and hypertrophy.

In conclusion, this study represents the first demonstration that ERK activation through MKP-1 down-regulation is involved in increased production of MCP-1 in adipocytes at the early stage of obesity. The data of this study suggest that MKP-1 activation may offer a novel therapeutic strategy to reduce the otherwise increased production of MCP-1 in hypertrophied

---

[4] A. Ito, T. Suganami, and Y. Ogawa, unpublished data.

- 94 -

## MKP-1 and Adipocyte Hypertrophy

adipocytes at the early stage of obesity and thus macrophage infiltration into the adipose tissue at the late stage of obesity.

## REFERENCES

1. Dandona, P., Aljada, A., and Bandyopadhyay, A. (2004) *Trends Immunol.* **25,** 4–7
2. Wellen, K. E., and Hotamisligil, G. S. (2005) *J. Clin. Investig.* **115,** 1111–1119
3. Berg, A. H., and Scherer, P. E. (2005) *Circ. Res.* **96,** 939–949
4. Weisberg, S. P., McCann, D., Desai, M., Rosenbaum, M., Leibel, R. L., and Ferrante, A. W., Jr. (2003) *J. Clin. Investig.* **112,** 1796–1808
5. Xu, H., Barnes, G. T., Yang, Q., Tan, G., Yang, D., Chou, C. J., Sole, J., Nichols, A., Ross, J. S., Tartaglia, L. A., and Chen, H. (2003) *J. Clin. Investig.* **112,** 1821–1830
6. Suganami, T., Nishida, J., and Ogawa, Y. (2005) *Arterioscler. Thromb. Vasc. Biol.* **25,** 2062–2068
7. Suganami, T., Tanimoto-Koyama, K., Nishida, J., Itoh, M., Yuan, X., Mizuarai, S., Kotani, H., Yamaoka, S., Miyake, K., Aoe, S., Kamei, Y., and Ogawa, Y. (2007) *Arterioscler. Thromb. Vasc. Biol.* **27,** 84–91
8. Chen, A., Mumick, S., Zhang, C., Lamb, J., Dai, H., Weingarth, D., Mudgett, J., Chen, H., MacNeil, D. J., Reitman, M. L., and Qian, S. (2005) *Obes. Res.* **13,** 1311–1320
9. Takahashi, K., Mizuarai, S., Araki, H., Mashiko, S., Ishihara, A., Kanatani, A., Itadani, H., and Kotani, H. (2003) *J. Biol. Chem.* **278,** 46654–46660
10. Cancello, R., Henegar, C., Viguerie, N., Taleb, S., Poitou, C., Rouault, C., Coupaye, M., Pelloux, V., Hugol, D., Bouillot, J. L., Bouloumie, A., Barbatelli, G., Cinti, S., Svensson, P. A., Barsh, G. S., Zucker, J. D., Basdevant, A., Langin, D., and Clement, K. (2005) *Diabetes* **54,** 2277–2286
11. Kamei, N., Tobe, K., Suzuki, R., Ohsugi, M., Watanabe, T., Kubota, N., Ohtsuka-Kowatari, N., Kumagai, K., Sakamoto, K., Kobayashi, M., Yamauchi, T., Ueki, K., Oishi, Y., Nishimura, S., Manabe, I., Hashimoto, H., Ohnishi, Y., Ogata, H., Tokuyama, K., Tsunoda, M., Ide, T., Murakami, K., Nagai, R., and Kadowaki, T. (2006) *J. Biol. Chem.* **281,** 26602–26614
12. Kanda, H., Tateya, S., Tamori, Y., Kotani, K., Hiasa, K., Kitazawa, R., Kitazawa, S., Miyachi, H., Maeda, S., Egashira, K., and Kasuga, M. (2006) *J. Clin. Investig.* **116,** 1494–1505
13. Johnson, G. L., and Lapadat, R. (2002) *Science* **298,** 1911–1912
14. Farooq, A., and Zhou, M. M. (2004) *Cell. Signal.* **16,** 769–779
15. Keyse, S. M. (2000) *Curr. Opin. Cell Biol.* **12,** 186–192
16. Sakaue, H., Ogawa, W., Nakamura, T., Mori, T., Nakamura, K., and Kasuga, M. (2004) *J. Biol. Chem.* **279,** 39951–39957
17. Bost, F., Aouadi, M., Caron, L., Even, P., Belmonte, N., Prot, M., Dani, C., Hofman, P., Pages, G., Pouyssegur, J., Le Marchand-Brustel, Y., and Binetruy, B. (2005) *Diabetes* **54,** 402–411
18. Rosen, E. D., and MacDougald, O. A. (2006) *Nat. Rev. Mol. Cell Biol.* **7,** 885–896
19. Kouyama, R., Suganami, T., Nishida, J., Tanaka, M., Toyoda, T., Kiso, M.,

20. Suganami, T., Mieda, T., Itoh, M., Shimoda, Y., Kamei, Y., and Ogawa, Y. (2007) *Biochem. Biophys. Res. Commun.* **354,** 45–49
21. Jinnouchi, K., Terasaki, Y., Fujiyama, S., Tomita, K., Kuziel, W. A., Maeda, N., Takahashi, K., and Takeya, M. (2003) *J. Pathol.* **200,** 406–416
22. Kamon, J., Naitoh, T., Kitahara, M., and Tsuruzoe, N. (2001) *Cell. Signal.* **13,** 105–109
23. Hosono, T., Mizuguchi, H., Katayama, K., Koizumi, N., Kawabata, K., Yamaguchi, T., Nakagawa, S., Watanabe, Y., Mayumi, T., and Hayakawa, T. (2005) *Gene (Amst.)* **348,** 157–165
24. Saitoh, T., Nakayama, M., Nakano, H., Yagita, H., Yamamoto, N., and Yamaoka, S. (2003) *J. Biol. Chem.* **278,** 36005–36012
25. Morita, S., Kojima, T., and Kitamura, T. (2000) *Gene Ther.* **7,** 1063–1066
26. Bueno, O. F., De Windt, L. J., Lim, H. W., Tymitz, K. M., Witt, S. A., Kimball, T. R., and Molkentin, J. D. (2001) *Circ. Res.* **88,** 88–96
27. Suganami, E., Takagi, H., Ohashi, H., Suzuma, K., Suzuma, I., Oh, H., Watanabe, D., Ojima, T., Suganami, T., Fujio, Y., Nakao, K., Ogawa, Y., and Yoshimura, N. (2004) *Diabetes* **53,** 2443–2448
28. Weisberg, S. P., Hunter, D., Huber, R., Lemieux, J., Slaymaker, S., Vaddi, K., Charo, I., Leibel, R. L., and Ferrante, A. W., Jr. (2006) *J. Clin. Investig.* **116,** 115–124
29. Skurk, T., Alberti-Huber, C., Herder, C., and Hauner, H. (2006) *J. Clin. Endocrinol. Metab.* **92,** 1023–1033
30. Camps, M., Nichols, A., and Arkinstall, S. (2000) *FASEB J.* **14,** 6–16
31. Fain, J. N., and Madan, A. K. (2005) *Int. J. Obes. (Lond.)* **29,** 1299–1307
32. Marumo, T., Schini-Kerth, V. B., and Busse, R. (1999) *Diabetes* **48,** 1131–1137
33. Yoshimura, H., Nakahama, K., Safronova, O., Tanaka, N., Muneta, T., and Morita, I. (2006) *Inflamm. Res.* **55,** 543–549
34. Barry, O. P., Mullan, B., Sheehan, D., Kazanietz, M. G., Shanahan, F., Collins, J. K., and O'Sullivan, G. C. (2001) *J. Biol. Chem.* **276,** 15537–15546
35. Tong, Z., Singh, G., and Rainbow, A. J. (2002) *Cancer Res.* **62,** 5528–5535
36. Manzano, R. G., Montuenga, L. M., Dayton, M., Dent, P., Kinoshita, I., Vicent, S., Gardner, G. J., Nguyen, P., Choi, Y. H., Trepel, J., Auersperg, N., and Birrer, M. J. (2002) *Oncogene* **21,** 4435–4447
37. Özcan, U., Cao, Q., Yilmaz, E., Lee, A. H., Iwakoshi, N. N., Ozdelen, E., Tuncman, G., Gorgun, C., Glimcher, L. H., and Hotamisligil, G. S. (2004) *Science* **306,** 457–461
38. Furukawa, S., Fujita, T., Shimabukuro, M., Iwaki, M., Yamada, Y., Nakajima, Y., Nakayama, O., Makishima, M., Matsuda, M., and Shimomura, I. (2004) *J. Clin. Investig.* **114,** 1752–1761
39. Lin, Y. W., Chuang, S. M., and Yang, J. L. (2003) *J. Biol. Chem.* **278,** 21534–21541
40. Lin, Y. W., and Yang, J. L. (2006) *J. Biol. Chem.* **281,** 915–926
41. Wu, J. J., Roth, R. J., Anderson, E. J., Hong, E. G., Lee, M. K., Choi, C. S., Neufer, P. D., Shulman, G. I., Kim, J. K., and Bennett, A. M. (2006) *Cell Metab.* **4,** 61–73
42. Prusty, D., Park, B. H., Davis, K. E., and Farmer, S. R. (2002) *J. Biol. Chem.* **277,** 46226–46232
43. Orlicky, D. J., DeGregori, J., and Schaack, J. (2001) *J. Lipid Res.* **42,** 910–915
44. Orlicky, D. J., and Schaack, J. (2001) *J. Lipid Res.* **42,** 460–466
45. Ross, S. A., Song, X., Burney, M. W., Kasai, Y., and Orlicky, D. J. (2003) *Biochem. Biophys. Res. Commun.* **302,** 354–358

Chiwata, T., Miyamoto, Y., Yoshimasa, Y., Fukamizu, A., Horiuchi, M., Hirata, Y., and Ogawa, Y. (2005) *Endocrinology* **146,** 3481–3489

– 95 –

# Circulating CD34-Positive Cell Number Is Associated With Brain Natriuretic Peptide Level in Type 2 Diabetic Patients

Sadanori Okada, md[1]
Hisashi Makino, md, phd[1]
Ayako Nagumo, md[1]
Takako Sugisawa, md, phd[1]
Muneya Fujimoto, md, phd[1]
Ichiro Kishimoto, md, phd[1]

Yoshihiro Miyamoto, md, phd[1]
Akie Kikuchi-Taura[2]
Toshihiro Soma, md[2]
Akihiko Taguchi, md, phd[3]
Yasunao Yoshimasa, md, phd[1]

Patients with type 2 diabetes often suffer from asymptomatic left ventricular (LV) injury, including increased LV mass, without apparent myocardial ischemia. The mechanisms underlying diabetic LV injury remain unclear; however, it has been suggested that endothelial dysfunction plays a role. Accumulating evidence indicates that bone marrow–derived endothelial progenitor cells (EPCs) contribute to neovascularization of ischemic tissue and endothelialization of denuded endothelium. Recent studies have shown that circulating bone marrow–derived immature cells, including CD34^{+} cells, contribute to the maintenance of the vasculature, both as a pool of EPCs and as the source of growth/angiogenesis factors (1). We hypothesized that circulating CD34^{+} cells might be associated with LV dysfunction in patients with type 2 diabetes. Therefore, we studied the correlation between circulating CD34^{+} cell levels and plasma brain natriuretic peptide (BNP) levels, an LV dysfunction marker, in type 2 diabetic patients.

## RESEARCH DESIGN AND METHODS

The institutional review board of the National Cardiovascular Center approved

this study, and all subjects provided informed consent. We examined 26 patients with type 2 diabetes (12 men and 14 women, duration of diabetes 16.1 ± 10.7 years) who were over 60 years of age (70.5 ± 6.4 years). Statin was given to nine subjects. ACE inhibitor or angiotensin receptor blocker was given to nine subjects, and thiazolidinedione was given to two subjects. Subjects were excluded from the study if they had known cardiovascular disease or chronic renal failure (defined as serum creatinine ≥180 μmol/l). No study subject showed hypokinesis by echocardiography or electrocardiogram change, indicating myocardial ischemia. Systolic (SBP) and diastolic (DBP) blood pressure and anthropometric parameters were determined. Blood samples were taken after 12-h fasting to measure circulating CD34^{+} cells, plasma BNP, fasting plasma glucose (FPG), and A1C. Circulating CD34^{+} cells were quantified by flow cytometry according to the manufacturer's protocol (ProCOUNT; Becton Dickinson Biosciences) as previously reported (2). BNP was quantified by enzyme immunoassay (Tohso, Tokyo, Japan). We further examined LV fractional shortening (LVFS), LV mass index (LVMI) (3), and peak flow velocity of the early filling wave (E), the late filling wave

(A), and the E/A-wave ratio (E/A) by echocardiography. All echocardiograms were performed by several expert physicians who were blinded to CD34^{+} cell level.

All statistical analyses were performed using JMP version 5.1.1 software (SAS Institute). Data are expressed as means ± SD. Comparisons of number of CD34^{+} cells by sex were made using the two-tailed unpaired $t$ test. Correlations between number of CD34^{+} cells and clinical parameters were assessed by univariate liner regression analysis and multiple regression analysis. LVMI and plasma BNP concentrations were analyzed after logarithmic transformation.

## RESULTS

FPG levels, A1C levels, and BMIs in the study subjects were measured to be 9.5 ± 2.6 mmol/l, 9.2 ± 1.8%, and 26.4 ± 4.3 kg/m$^2$, respectively. A total of 88% of the patients had hypertension (SBP 142 ± 18 mmHg, DBP 75.7 ± 13.5 mmHg). Plasma BNP levels were measured to be 95 ± 319 pg/ml. Although it has been reported that the level of BNP ≥100 pg/ml has a sensitivity of 90% of diagnosing congestive heart failure (CHF) in patients with CHF symptoms (4), none of the subjects in this study, including subjects with ≥100 pg/ml of BNP, showed symptoms of CHF. The level of circulating CD34^{+} cells was measured to be 0.76 ± 0.39 cells/μl, and there was no significant difference between sexes. The range of LVMI was 73.3–340.2, and 11 subjects applied to the definition of LV hypertrophy (LVMI ≤131 in men and ≤100 in women) (3).

Plasma BNP levels had a significant inverse correlation with the number of circulating CD34^{+} cells (Fig. 1A), whereas FPG, A1C, BMI, SBP, DBP, and age showed no significant correlations. There was a significant correlation between the number of circulating CD34^{+} cells and LVMI by echocardiography (Fig. 1B). LVFS and E/A were not associated with circulating CD34^{+} cell numbers (LVFS $r = -0.07$, $P = 0.72$; E/A $r = -0.11$, $P = 0.59$). There was also a significant correlation between BNP levels and LVMI ($r = 0.59$, $P = 0.001$).

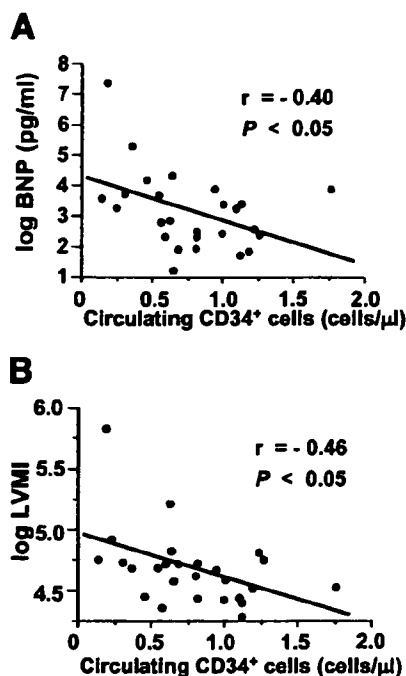In multiple regression analysis, the

**A**



**B**



**Figure 1**—*Correlation between CD34$^+$ cell numbers and plasma BNP levels (A) and correlation between CD34$^+$ cell numbers and LVMI (B) in type 2 diabetic patients (n = 26).*

level of CD34$^+$ cells was an independent correlate of both BNP ($\beta = -1.64$, $P = 0.017$) and LVMI ($\beta = -0.337$, $P = 0.031$) in the model including age, A1C, SBP, BMI, and medication (ACE inhibitor/angiotensin receptor blocker, statin, and thiazolidinedione).

**CONCLUSIONS**— In this study, circulating CD34$^+$ cell number was found to significantly correlate with plasma BNP level, a marker of LV dysfunction. To the best of our knowledge, this is the first report that circulating bone marrow–derived cells are associated with diabetic LV abnormality. Circulating CD34$^+$ cell numbers also significantly correlated with LVMI, whereas they did not correlate with LVFS (an LV systolic function marker) or E/A (an LV diastolic function marker). LV hypertrophy is a well-known predictor of cardiovascular events independent of coronary artery disease. The Framingham Heart Study identified an association be-

tween diabetes and increased LV wall thickness and mass (5). Although the precise mechanisms underlying the association between diabetes and LV hypertrophy remain unknown, our results suggest that reduced circulating CD34$^+$ cell numbers may be involved in the progression of LV hypertrophy in diabetic patients. However, further investigations are necessary to demonstrate this hypothesis.

We measured the level of CD34$^+$ cells in this study but not the levels of circulating CD34$^+$/kinase insert domain receptor (KDR)$^+$ cells that are regarded as EPCs. Circulating CD34$^+$ cell levels are associated with ischemic stroke (6), and administration of CD34$^+$ cells ameliorates cerebral ischemia in mice (7). This indicates that CD34$^+$ cells may be involved in cardiovascular disease. Indeed, another recent report indicated that levels of circulating CD34$^+$ cells are more strongly correlated with cardiovascular risk than levels of EPCs (8). Therefore, our results suggest that measurement of CD34$^+$ cells may provide an indicator for diabetic LV hypertrophy.

Our study had several limitations. First, the study was performed only by cross-sectional analysis; therefore, a prospective study is needed to clarify whether circulating CD34$^+$ cell numbers predict LV injury in diabetic patients. Second, although systemic blood pressure did not significantly associate with CD34$^+$ cell numbers, further investigation of normotensive diabetic patients is needed to exclude the possible effects of hypertension on circulating CD34$^+$ cell numbers, as most of the subjects in this study were hypertensive. Despite this caveat, these results may be of practical use in elderly patients with type 2 diabetes, as hypertension is a very common comorbid condition in this population.

In conclusion, reduced circulating CD34$^+$ cell numbers are significantly associated with plasma BNP concentration and LVMI in elderly patients with type 2 diabetes. These results suggest that decreased circulating CD34$^+$ cells may be involved in LV hypertrophy and that measurement of circulating CD34$^+$ cell num-

bers may be useful for the identification of diabetic patients at high risk of LV injury.

**References**
1. Majka M, Janowska-Wieczorek A, Ratajczak J, Ehrenman K, Pietrzkowski Z, Kowalska MA, Gewirtz AM, Emerson SG, Ratajczak MZ: Numerous growth factors, cytokines, and chemokines are secreted by human CD34(+) cells, myeloblasts, erythroblasts, and megakaryoblasts and regulate normal hematopoiesis in an autocrine/paracrine manner. *Blood* 97:3075–3085, 2001
2. Kikuchi-Taura A, Soma T, Matsuyama T, Stern DM, Taguchi A: A new protocol for quantifying CD34(+) cells in peripheral blood of patients with cardiovascular disease. *Tex Heart Inst J* 33:427–429, 2006
3. Devereux RB, Reichek N: Echocardiographic determination of left ventricular mass in man: anatomic validation of the method. *Circulation* 55:613–618, 1977
4. McCullough PA, Nowak RM, McCord J, Hollander JE, Herrmann HC, Steg PG, Duc P, Westheim A, Omland T, Knudsen CW, Storrow AB, Abraham WT, Lamba S, Wu AHB, Perez A, Clopton P, Krishnaswamy P, Kazanegra R, Maisel AS, BNP multinational study investigators: B-type natriuretic peptide and clinical judgment in emergency diagnosis of heart failure: analysis from Breathing Not Properly (BNP) Multinational Study. *Circulation* 106: 416–422, 2002
5. Galderisi M, Anderson KM, Wilson PW, Levy D: Echocardiographic evidence for existence of a distinct diabetic cardiomyopathy (the Framingham Heart Study). *Am J Cardiol* 68:85–89, 1991
6. Taguchi A, Matsuyama T, Moriwaki H, Hayashi T, Hayashida K, Nagatsuka K, Todo K, Mori K, Stern DM, Soma T, Naritomi H: Circulating CD34-positive cells provide an index of cerebrovascular function. *Circulation* 109:2972–2975, 2004
7. Taguchi A, Soma T, Tanaka H, Kanda T, Nishimura H, Yoshikawa H, Tsukamoto Y, Iso H, Fujimori Y, Stern DM, Naritomi H, Matsuyama T: Administration of CD34+ cells after stroke enhances neurogenesis via angiogenesis in a mouse model. *J Clin Invest* 114:330–338, 2004
8. Fadini GP, de Kreutzenberg SV, Coracina A, Baesso I, Agostini C, Tiengo A, Avogaro A: Circulating CD34+ cells, metabolic syndrome, and cardiovascular risk. *Eur Heart J* 27:2247–2255, 2006

Amino Acids

# Adrenomedullin: molecular mechanisms and its role in cardiac disease

## Review Article

**B. Yanagawa and N. Nagaya**

Department of Regenerative Medicine and Tissue Engineering, National Cardiovascular Center Research Institute, Osaka, Japan

**Summary.** Adrenomedullin (AM) is a potent, long-lasting vasoactive peptide originally isolated from human pheochromocytoma. Since its discovery, serum and tissue AM expression have been shown to be increased in experimental models and in patients with cardiac hypertrophy, myocardial infarction and end-stage heart failure with several beneficial effects. Considerable evidence exists for a wide range of autocrine, paracrine and endocrine mechanisms for AM which include vasodilatory, anti-apoptotic, angiogenic, anti-fibrotic, natriuretic, diuretic and positive inotropic. Thus, through regulation of body fluid or direct cardiac mechanisms, AM has additive and beneficial effects in the context of heart disease. Notable molecular mechanisms of AM include cyclic adenosine monophosphate, guanosine-3′,5′-monophosphate, PI3K/Akt and MAPK-ERK-mediated cascades. Given the endogenous and multifunctional nature of AM, we consider this molecule to have great potential in the treatment of cardiovascular diseases. In agreement, early experimental and preliminary clinical studies suggest that AM is a new and promising therapy for cardiovascular diseases.

**Keywords:** Adrenomedullin – Heart disease – Signaling

## Introduction

Adrenomedullin (AM) is a member of the calcitonin gene-related peptide (CGRP) family, which was originally discovered in human adrenal medulla as a hypotensive factor produced by pheochromocytoma cells (Kitamura, 1993). This molecule is synthesized as an immature 53-amino acid precursor and modified by amidation into a mature 52-amino-acid peptide with an intramolecular disulfide bond, sharing slight homology with CGRP and amylin. Since its discovery, this molecule has subsequently been found in plasma and in a variety of tissues including the vasculature, lungs, heart and adipose tissue (Ichiki, 1994; Saito, 1987; Fukai, 2004). In the heart, AM is present in ventricular tissue and is particularly abundant in rat atria (Ichiki, 1994; Sakata, 1994). Although mainly produced

by vascular endothelial cells, vascular smooth muscle cells and macrophages, AM can also be produced by fibroblasts, adipocytes and cardiac myocytes (Sugo, 1994, 1994a; Kubo, 1998). Earlier studies have shown that plasma AM levels are increased in patients with heart failure (Nishikimi, 1995). Since then, increased AM has been detected in hearts of patients with acute myocardial infarction, hypertension, chronic heart failure and pulmonary hypertension.

In this review, although we will refer to studies involving AM signaling in various cell types and diseases settings, our focus on the role of AM in cardiovascular illness. Certainly, the critical importance of AM in cardiovascular development is highlighted by the severe tissue edema and cardiac abnormalities seen in AM-null mice (Caron, 2001). Here, we review the current literature regarding the molecular mechanisms of AM, investigate its role in cardiovascular disease and look ahead to the potential of AM in the treatment of heart disease.

## Signaling

Since its discovery, the role of AM in heart failure and its molecular mechanisms of action have been an intense area of study. Signaling studies of AM have largely been performed in endothelial and smooth muscle cell types with calcium- and cAMP-mediated cascades having been identified as the predominant mechanisms of AM action, respectively. Here, we will review the AM receptors and AM signaling pathways including cyclic adenosine 3′,5′-monophosphate (cAMP) and calcium, cyclic guanosine 3′,5′-monophosphate (cGMP), phosphatidylinositol